W. Becker

Becker & Hickl GmbH

Bigger and Better Photons
The Road to Great FLIM Results

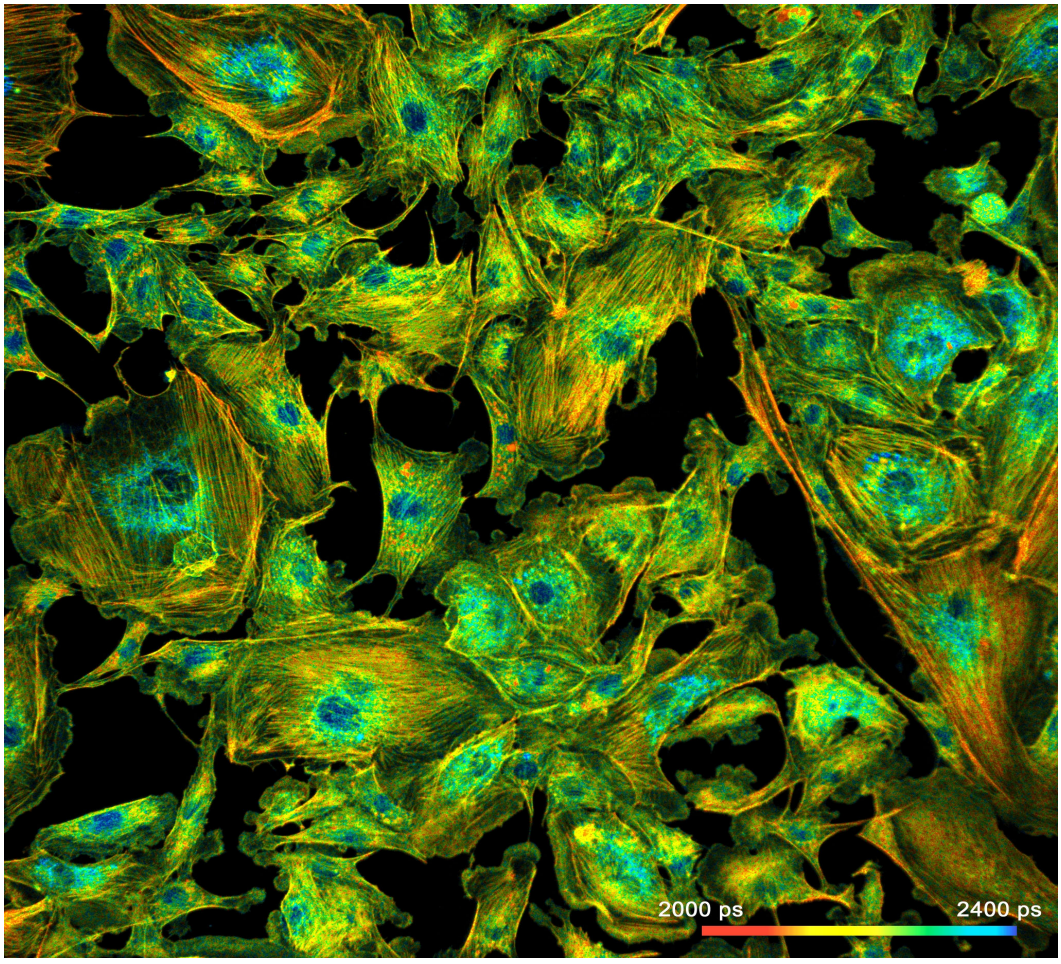

2023

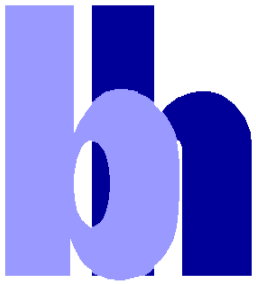

Becker & Hickl GmbH
Nunsdorfer Ring 7-9
12277 Berlin
Germany
Tel. +49 / 30 / 787 56 32
FAX +49 / 30 / 787 57 34
http://www.becker-hickl.com
email: info@becker-hickl.com

May 2023

Contents

Bigger and Better Photons: The Road to Great FLIM Results

Wolfgang Becker, Becker & Hickl GmbH

Abstract: These pages are an attempt to help existing and future users of the bh FLIM technique obtain the best possible results from their FLIM experiments. The first part of the brochure explains the principle of TCSPC FLIM, and gives an impression of the photon distributions recorded. It shows that the signal-to-noise ratio of the measured lifetimes depends, in first order, on the number of photons recorded. The following sections focus on optimising the photon number without increasing the photostress imposed to the sample. We discuss the influence of excitation power, acquisition time, collection efficiency, numerical aperture, focusing precision, alignment accuracy, and detector efficiency. The next section concentrates on photon efficiency. It considers TCSPC timing parameters, counting background, number of pixels, the influence of the instrument-response function, and the challenges of multi-exponential decay functions. The last section is dedicated to data analysis. All conclusions made in this brochure are demonstrated on real measurement data recorded under realistic conditions.

Great FLIM Images

What makes a great FLIM image? Well, it should have perfect spatial resolution, it should be recorded into a sufficiently high number of pixels, it should have high contrast, low background, no out-of-focus blur, and it should display the fluorescence lifetime at a high signal-to-noise ratio. Just as the image shown below. An experienced FLIM user will probably add that just recording the fluorescence lifetime is not enough, and the entire decay function should be recorded in every pixel.

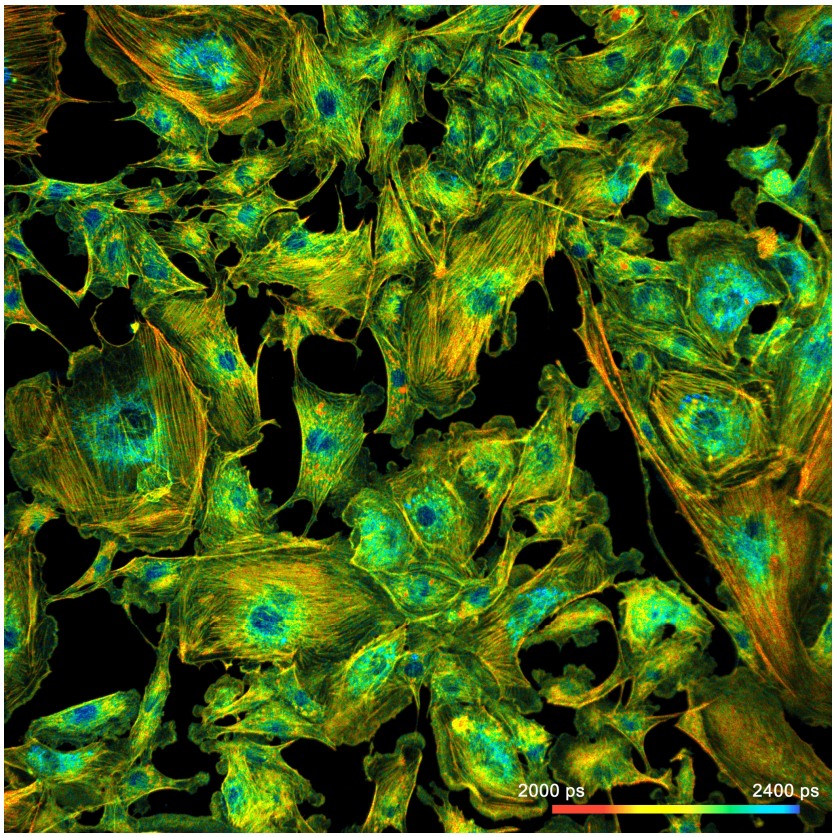

Fig. 1: FLIM image of a BPAE sample. 2048 x 2048 pixels, decay functions recorded into 256 time channels. bh DCS-120 confocal FLIM system, bh SPCImage FLIM data analysis software.

Why do FLIM images published in scientific papers rarely look like the image above? There is actually no reason for that. All that has to be done is to use perfectly aligned optics, the right microscope lens, perfect focusing, the right excitation and detection wavelengths, the right detector, and a little bit of patience. Some comprehension of the signal-processing principles of FLIM may be helpful as well. This is something every FLIM user can achieve.

This article shows what is important to obtain great FLIM results. Most of the advice given on these pages will be trivial. However, it is just the sum of these trivial things that makes the difference between a mediocre lifetime image and a perfect FLIM result.

TCSPC FLIM Results are Photon Distributions

Principle of TCSPC FLIM

The road to perfect FLIM results starts with the understanding that a TCSPC FLIM result is a photon distribution [1]. The basic principle of the recording process is shown in Fig. 2.

The sample is scanned by a high-frequency pulsed laser beam, single photons of the emitted fluorescence light are detected, and the arrival time, t, of each photon in the laser pulse period is determined by the TCSPC system. In parallel, the TCSPC system determines the spatial coordinates, x,y, of the laser beam in the moment of the photon detection. From these data, the distribution of the photons over the spatial coordinates and the times of the photons is built up. This photon distribution is the desired lifetime image: It is a data array of x × y pixels, each of which contains a fluorescence decay function in a large number of consecutive time channels. See Fig. 2, right. A detailed description of the recording process and its various extensions can be found in [2].

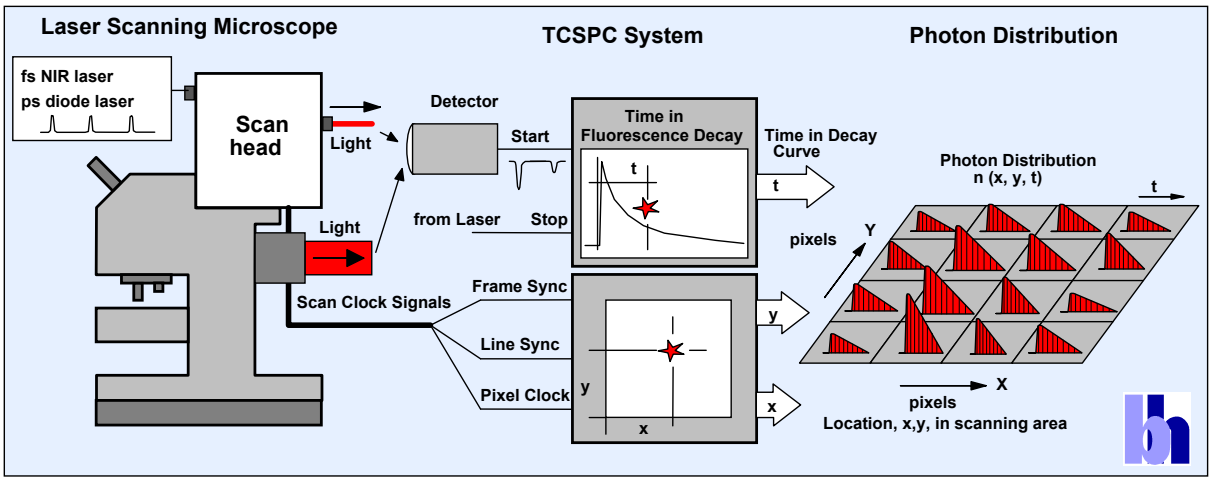

Fig. 2: Principle of TCSPC FLIM

Fig. 3 gives an impression of the photon distribution recorded by FLIM. The figure shows an image area of 8 horizontal x 128 vertical pixels. Each pixel has 256 time channels, containing decay data of this pixel. Of course, a real FLIM image has a much higher number of pixels. FLIM formats of 512 x 512 pixels with 256 to 1024 time channels are used routinely, and formats of 2048 x 2048 pixels with 256 time channels have been demonstrated [2].

To an inexperienced user the distribution shown in Fig. 3 may look very 'noisy': The fluorescence decay in the individual pixels can barely be seen. Of course, the 'noise' is not caused by any noise of

the detector or the TCSPC electronics. It is simply an effect of photon statistics. The reason that the noise is so high is that the photons are distributed over a large number of pixels and time channels. Consequently, the number of photons in the individual pixels, and, especially, in the individual time channels if each pixel is low. So, how can the 'noise' in the photon distribution be reduced? The only way is to record more photons, see Fig. 4.

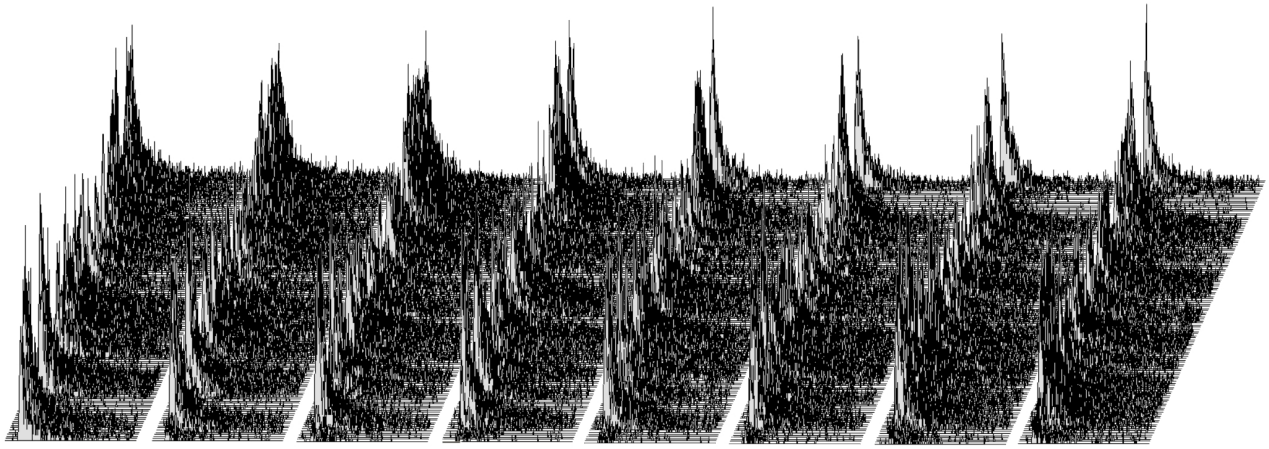

Fig. 3: The photon distribution of TCSPC FLIM. The figure represents an image area of X × Y = 8 × 128 pixels. Each pixel has 256 time channels, each containing the photons at consecutive times within the fluorescence decay.

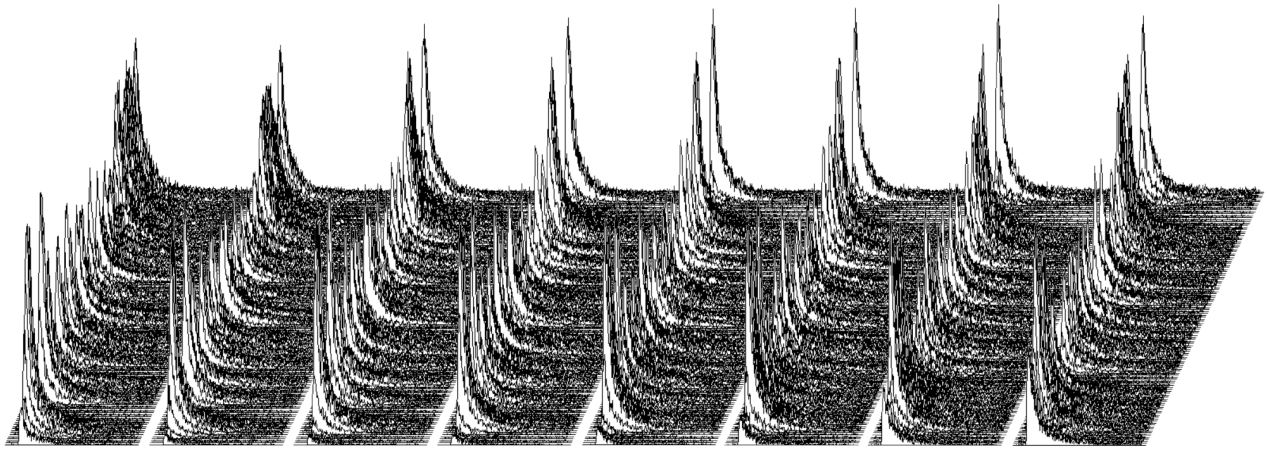

Fig. 4: The same photon distribution as shown in Fig. 3, but after recording 10 times more photons. The signal-to-noise ratio is 3.1 times higher, and the fluorescence decay curves in the individual pixels stand out clearly.

Signal-to-Noise Ratio

What is the signal-to-noise ratio of a fluorescence lifetime derived from such data? We obtain the answer from a simple gedankenexperiment.

By definition, the fluorescence lifetime, τ, is the average time a molecule stays in the excited state. When a molecule gives off a photon it means that it returned from the excited state. The FLIM system detects the individual photons and determines their times, t, after the excitation pulse, see Fig. 5, a and b. When the FLIM system detects a large number of such photons their average arrival time after the excitation pulse is the average time of the molecules in the excited state and thus the fluorescence lifetime, see Fig. 5 c. Although the FLIM hardware normally does not calculate the average arrival time directly, it is implicitly present in the photon distribution.

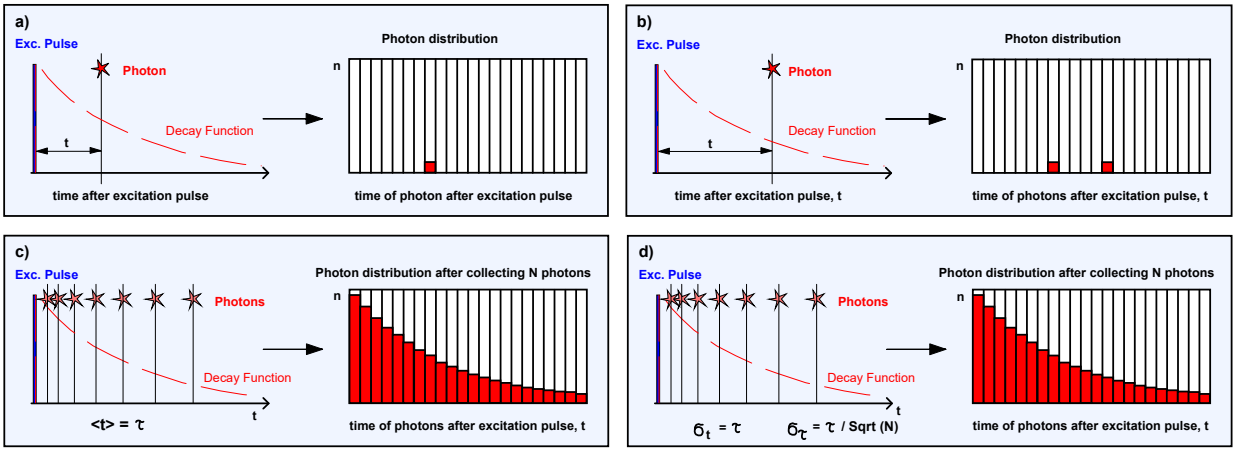

Fig. 5, a and b: Detection of photons and buildup of the photon distribution over the time after excitation, t. c: Photon distribution after the detection of N photons. The average arrival time after the excitation, <t>, is the fluorescence lifetime, τ. d: The standard deviation, σ_t, of the arrival times, t, is τ. The standard deviation, σ_τ, of the average arrival times is τ / SQRT(N).

What is the signal-to-noise ratio of the average arrival time? The standard deviation, σ_τ, of the arrival time of the individual photons is identical with the fluorescence lifetime, τ, itself. This is a property of the exponential function. If we average the arrival times for a number of photons, N, the standard deviation, σ_τ, of the result decreases with the square root of N, see Fig. 5, d. The signal-to-noise ratio, i.e. the ratio of τ divided by its standard deviation, σ_τ after the detection of N photons is therefore:

$$SNR_\tau = \tau / \sigma_\tau = SQRT\ (N)$$

That means the standard deviation at which the fluorescence lifetime can be obtained is simply the square root of the number of photons in the decay curve [20]. This is a remarkable result in several respects. First, the signal-to-noise ratio for the pixel lifetime is the same as for the *pixel intensity*. This invalidates the widespread opinion that FLIM needs more photons (and thus more acquisition time) than steady-state imaging. Second, the signal-to-noise ratio depends *only* on N. In particular, is does not depend on the number of time channels into which the fluorescence decay is recorded. In other words, you can increase the number of time channels to improve the time resolution or to reduce sampling artefacts without compromising the signal-to-noise ratio. Third, because the SNR depends on N only, the only way to increase the lifetime accuracy is to increase N. That means you either have to decrease the number of pixels - which you normally don't want - or record more photons. Getting these photons recorded is the key to a good FLIM result, and it is the subject of the next section.

The First Moment of the Photon Distribution

As explained above, the fluorescence lifetime of a single-exponential decay (or of a single-exponential approximation of the decay) can be obtained by calculating the average arrival time of the photons. If the individual arrival times of the photons are not available the average arrival time can be obtained from the complete photon distribution by calculating the 'First Moment', M1 [21]:

$$M1 = \frac{1}{N}\sum tn(t)$$

The time, t, in the above equation is the time of the photons in the observation time interval of the FLIM system, not the time after the excitation pulse. Therefore, the time of excitation (in practice the first moment of the IRF) has to be subtracted to obtain τ:

$$\tau = M1_{fluorescence} - M1_{IRF}$$

The method is illustrated in Fig. 2. The blue dots are the photon numbers in the individual time channels, the green curve is the IRF, the red curve is the hypothetical fluorescence decay function calculated by convoluting an exponential function, $e^{-t/\tau}$, with the IRF.

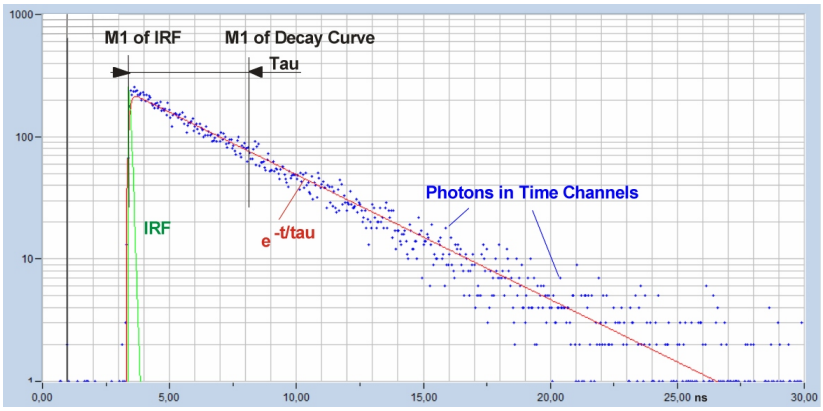

Fig. 6: First-moment calculation of fluorescence lifetime. The lifetime is the difference of the first moment of the fluorescence and the first moment of the IRF.

The first-moment technique delivers single-exponential decay times at an ideal signal-to-noise ratio. However, it does not deliver the parameters of multi-exponential decay functions, and it does not deliver correct decay times if the recording contains background counts or if only a part of the decay functions is in the observation-time interval of the TCSPC system. Therefore it has almost entirely been replaced by curve-fitting techniques. Nevertheless, the first moment technique has its benefits: It works reliably at very low photon numbers, it is suitable for fast lifetime determination in online-FLIM applications, and, most importantly, it provides a way to estimate the signal-to-noise ratio of FLIM both under ideal and non-ideal conditions. We will make use of this capability in later sections of this brochure.

An experimental verification of the SQRT (N) relation is shown in Fig. 7. A dye solution was scanned with different acquisition time in order to obtain FLIM images containing about 200, 1600, and 9000 photons per pixel. Typical decay curves are show in the top row of Fig. 7. The second row shows histograms of the fluorescence lifetime in the individual pixels, as it is obtained by first-moment analysis. The σ_τ values and the σ / τ = SNR values are indicated in the histograms. As can be seen from these values, σ / τ is indeed very close to SQRT (N). The bottom row of Fig. 7 shows histograms of the lifetimes obtained by an MLE (maximum-likelihood estimation) fit. The histograms of the lifetime obtained from the MLE fit are a bit broader than those from the moment analysis. But also the MLE results are close to the ideal SNR of SQRT (N).

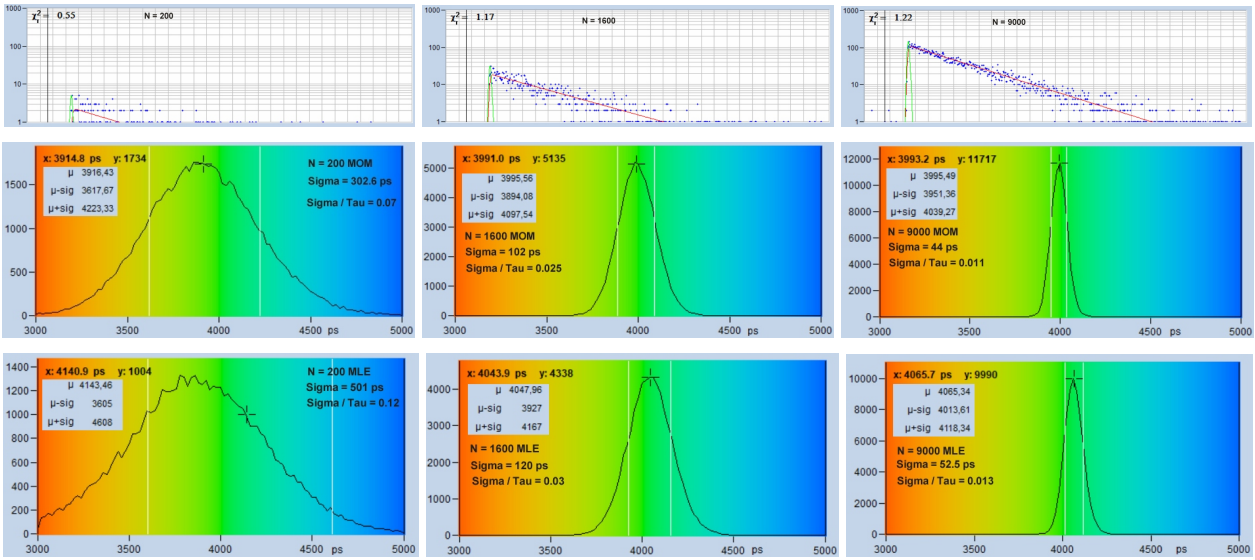

Fig. 7: Verification of the SQRT (N) relation. Top row: Decay curves from single pixels of FLIM data from a Rhodamine 110 dye solution. Left to right: N = 200 photons, N = 1600 photons, N = 9000 photons. Second row: Histograms of the lifetimes obtained by first-moment analysis. Bottom row: Histograms of the lifetimes obtained by MLE analysis.

Photon Efficiency

The fact that a photon was detected does not necessarily mean that it efficiently contributes to the accuracy of the lifetime measurement. It can be lost by unfavourably selected timing parameters in the TCSPC module, its detection time can be impaired by uncertainty in the detector transit time, or there may be photons from background signals which add unwanted noise to the photon distribution. In all these cases the SNR of the obtained lifetimes becomes smaller than the ideal value, SQRT(N). The situation can be described by a 'Photon Efficiency', E. The reciprocal of E tells how many photons the non-ideal system needs in comparison to the ideal system to reach the same signal-to-noise ratio. Since the SNR scales with the square root of the photon number the photon efficiency can also be written

$$E = (SNR_{real} / SNR_{ideal})^2$$

The photon efficiency, E, is the square of the 'Figure of Merit' that is sometimes used to compare the efficiency of different lifetime-measurement techniques [13, 19]. A correctly configured TCSPC system working under optimal conditions has a photon efficiency close to one. Reaching the ideal photon efficiency will be the subject of section 'Maximising the Photon Efficiency'.

Increasing the Number of Photons

Excitation Power

When a FLIM user wishes to increase the photon rate the first idea is usually to increase the excitation power. This is certainly an efficient way to get more photons. However, it is not always a useful way to obtain better FLIM results. FLIM is usually performed on samples with low fluorophore concentration. The reason is that molecular effects can only be seen if the fluorophore itself does not have noticeable effects on the viability of the cells or on their metabolic functions. In addition, the fluorophores may have low quantum efficiency. At increased excitation power the molecules have to perform more excitation-emission cycles, with the result that photobleaching, formation of radicals, laser-induced lifetime changes, photodamage, or even utter destruction of the sample occurs. The imaging process is then no longer non-invasive, and the FLIM results become meaningless. The

options of increasing the laser power are therefore limited [11]. A few examples of invasive effects are shown in Fig. 8.

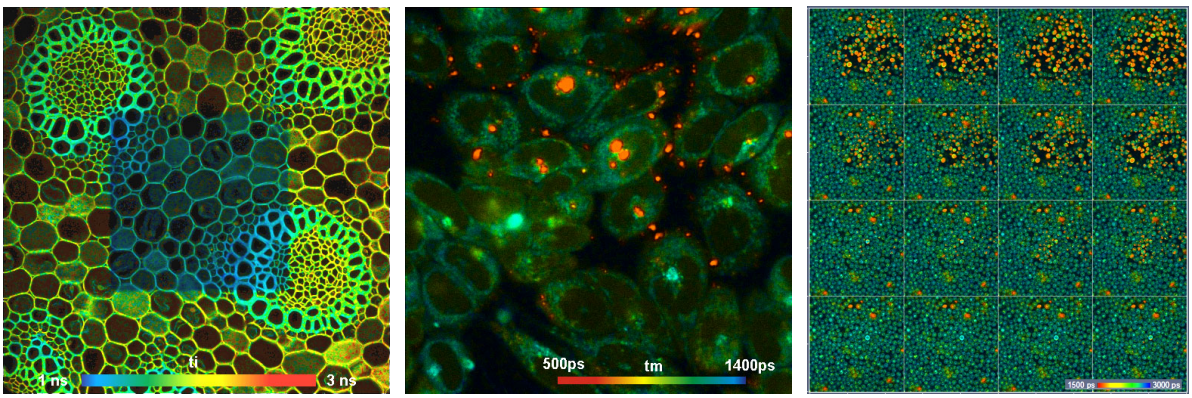

Fig. 8: Left: Convallaria image, region in the centre scanned with 405 nm laser. Middle: Two-photon NADH image of live cells. In the bright red spots photodamage has occurred, revealing itself by spots of very fast decay. Right: Temporal Mosaic FLIM of yeast cells, 2-photon excitation at 780 nm. Recording started in the element lower left, and proceeds to the upper right of the array. Destruction starts in elements 8 and 9 and continues until element 16.

Acquisition Time

Different than increasing the excitation power, increasing the acquisition time usually *is* an option. Damage effects are highly nonlinear. Often a sample can be scanned for a long time at a power that is only moderately lower than the damage threshold. Therefore, the options of increasing the photon number are indeed real. All that is needed is patience of the experimentator. An example is shown in Fig. 9. The left image was recorded with 1 minute acquisition time, the right one with 2 minutes. Not surprisingly, the right image contains 2 times more photons. As expected, it also provides a 1.4 times better SNR of the lifetime, see lifetime histograms underneath the images.

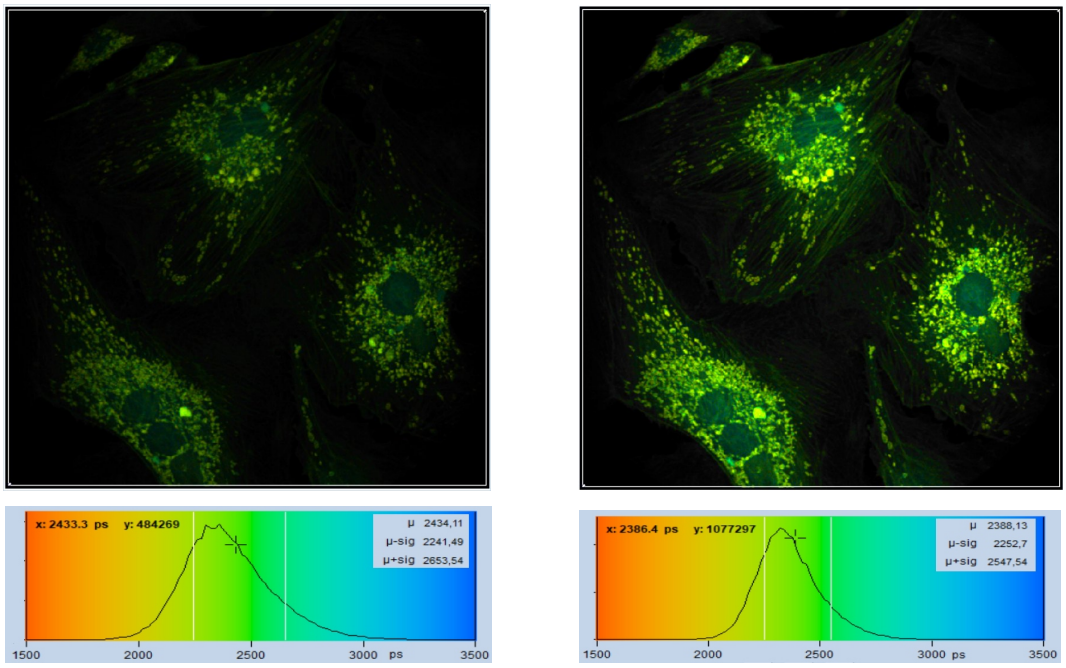

Fig. 9: Same sample imaged with different acquisition time. Left 1 minute, right 2 minutes. Image format 512x512 pixels, 1024 time channels.

Although the dependence of the photon number (and thus of the lifetime accuracy) on the acquisition time is trivial, it is often not realised by FLIM users. Especially users coming from conventional intensity-based imaging tend to stop the acquisition when a reasonable SNR of the *intensity image* has been reached. However, there is a fallacy. An intensity image starts to look good when it contains no more than a few 10 photons per pixel. The SNR of such an image may be enough to distinguish different fluorophores but it is not enough to derive the desired molecular information from the fluorescence lifetimes. Therefore, make sure that you run the acquisition for a sufficiently long period of time. SPCM provides a number of options to check the photon number during the acquisition. You can display a decay curve in a selected pixel or in an region of interest, you can display the photon number in the brightest pixel and in a selected pixel, and you can display a lifetime image online. Please see Fig. 10. With these options you should be able to decide whether the data recorded up to this point are good enough for further analysis. If in doubt record longer.

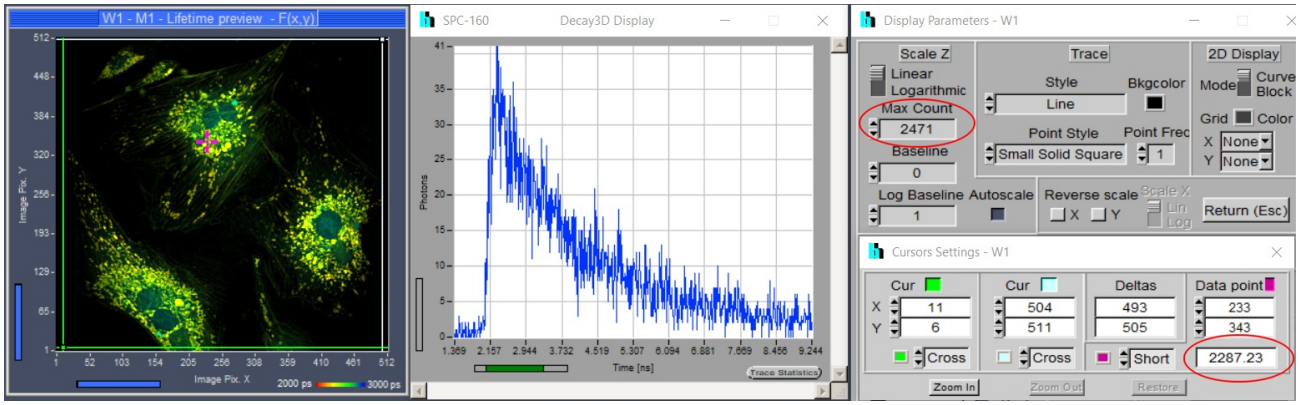

Fig. 10: SPCM functions help a user decide whether enough photons have been recorded. Left to right: Online lifetime image, decay curve at selected position, photon number in brightest pixel (top) and photon number at position of data point.

It is sometimes objected that long acquisition time is not an option when physiological changes are to be observed. This is not entirely correct, however, if appropriate multidimensional TCSPC techniques are used. Please see [2, 12].

Microscope Lens

The numerical aperture of the microscope lens has a significant influence of the detection efficiency. Fluorescence is emitted isotropically, and only a part of it is collected by the microscope lens. Theoretically, the collection efficiency increases with the square of the numerical aperture. That means a lens with NA = 1.25 should collect 6 times more photons than a lens with NA = 0.5. In practice the difference is smaller because high-NA lenses have more optical elements and less transmission. Nevertheless, the difference in collection efficiency is striking. An example is shown in Fig. 11. Both images were recorded by one-photon excitation and confocal detection. The left image was recorded with an x20 air lens of NA = 0.5, the right image was recorded with an x63 oil immersion lens, NA = 1.25. The image recorded with the high-NA lens contains three times the photons as the image recorded at low NA.

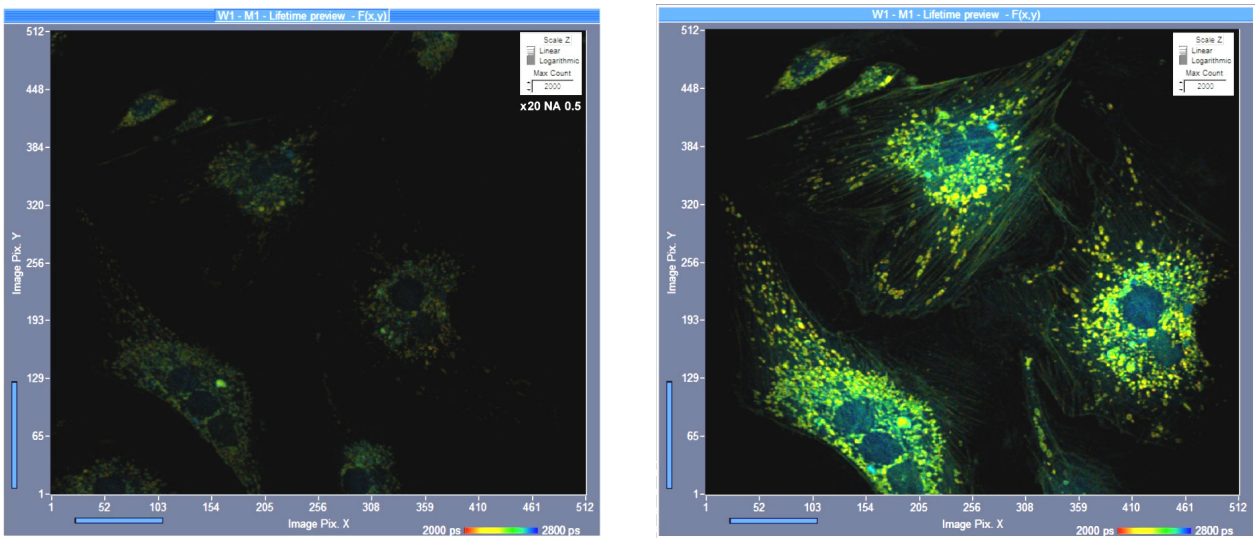

Fig. 11: FLIM image recorded with lenses of different NA, same intensity scale. One-photon excitation, confocal detection. Left: X20 air, NA=0.5. Right: X63 oil immersion, NA=1.25.

Focusing

Poor focusing is usually considered just a source of sub-optimal spatial resolution. However, it has also a significant effect on the detection efficiency. An example is shown in Fig. 12. Both images were recorded by confocal scanning, and with the same pinhole size and the same acquisition time. The left image is slightly defocused. Still, the image definition is only slightly impaired. The right image is perfectly in focus. It can easily be seen that the correctly focused image is brighter. Compared to the defocused image, the number of photons is about 1.5 higher. The differences are often not noticed because the FLIM system displays intensity-normalised images. (This is done because intensities can vary over orders of magnitude) Therefore, when you do the final focusing in the 'Preview' mode, take a few seconds to optimise the focus with the autoscale function turned off.

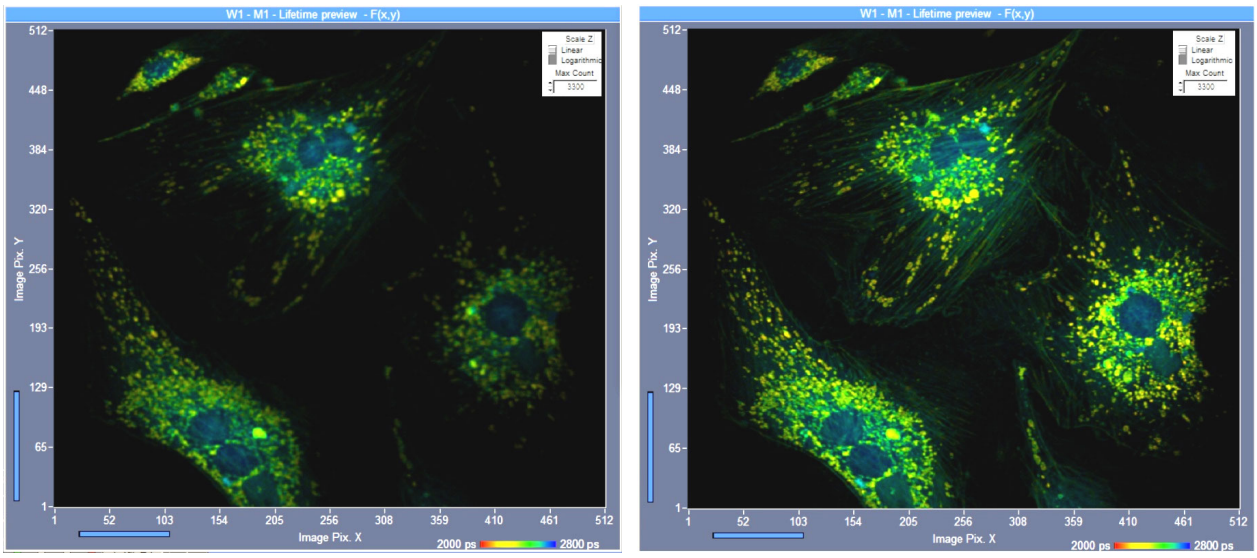

Fig. 12: Slightly defocused image (left) and perfectly focused image and (right). Same intensity scale, one-photon excitation, confocal detection. Although the image definition is only slightly impaired in the defocused image the photon number is only 60 % of the photon number in the perfect image. Image format 512 x 512 pixels, 1024 time channels.

Alignment of the Optical System

The alignment of the optical system has a massive influence on the detection efficiency. This is especially the case for confocal systems. Confocal alignment is extremely critical. There is virtually no confocal system that stays in perfect alignment over a longer period of time. An example is shown in Fig. 13. The image on the left was recorded with the pinhole alignment slightly off. Misalignment on this level is found in almost any confocal system. Usually, it remains unnoticed because the image definition is virtually unimpaired. However, a comparison with the image from the perfectly aligned system (Fig. 13, right) shows that there is a noticeable loss in the number of recorded photons. Misalignment on a level that even causes visible degradation in image definition can lead to a massive loss in photon number. Efficiency degradation by an order of magnitude and more is not unusual in these cases.

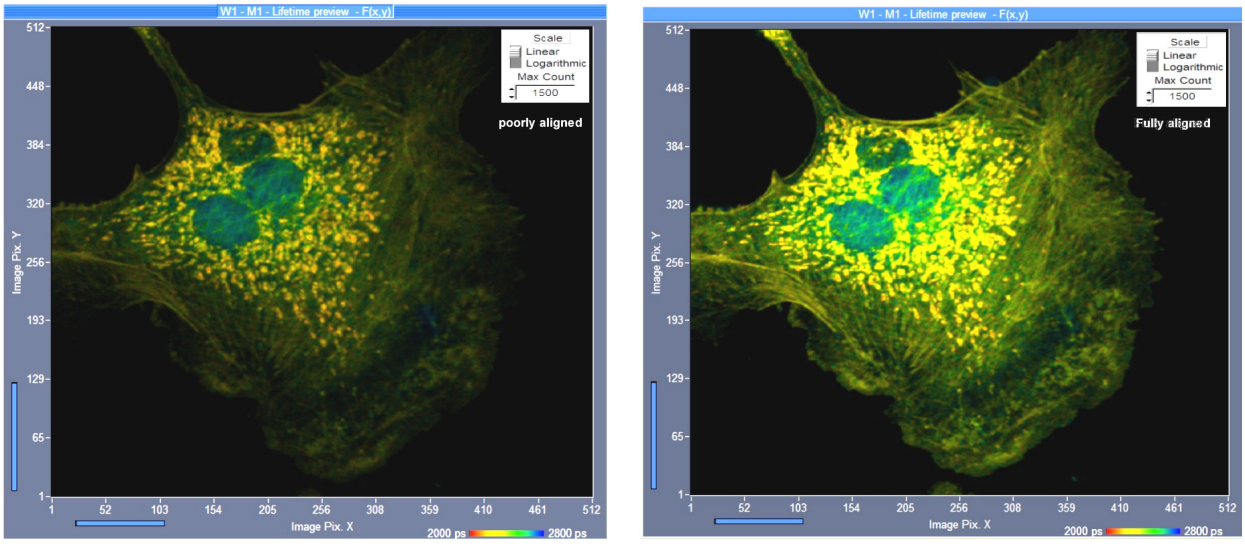

Fig. 13: Effect of confocal alignment. Left: Slightly misaligned. Right: Perfectly aligned. Although the misalignment does not yet lead to a visible loss in image definition it causes a loss of 50% of the photons.

Misalignment can even play a role in multiphoton systems with non-descanned detection. Although the detection light path of these systems is robust and rarely goes out of alignment the excitation path is critical. The femtosecond laser of a multiphoton microscope needs to be free-beam coupled into the scanner. This provides plenty of ways the light path can get out of alignment. The laser is then no longer centred on the back aperture of the microscope lens. As a result, the focus quality degrades, and the excitation efficiency decreases. Photobleaching and photodamage do not always decrease by the same ratio, especially if the sample has some absorption at the fundamental wavelength of the laser. Also multiphoton systems should therefore be re-aligned from time to time. This can easily be done by checking the position of the laser beam in the back aperture of the objective lens and bringing it back to the centre.

Detector

For many years, laser scanning microscopes and, in particular, FLIM systems have been built with conventional photomultipliers (PMTs). PMTs have large active areas, extremely low dark count rates per square-millimeter of active area, and sufficient gain and speed to detect single photons. The photocathodes of PMTs with conventional photocathodes have about 20% quantum efficiency. However, not every photoelectron emitted by the cathode enters the amplification system and delivers

a useful single-electron pulse. The net efficiency is therefore on the order of 15%. The efficiency increased with the introduction of PMTs with GaAsP cathodes. These cathodes have a quantum efficiency of almost 50%. GaAsP PMTs, such as the Hamamatsu H7422, have been used for FLIM for a number of years. However, the instrument response (IRF) width of these detectors is on the order of 250 to 350 ps, which is not sufficient for high-end FLIM applications. The situation changed entirely with the introduction of the R10467-40 hybrid PMT of Hamamatsu. The principle of the hybrid PMT guarantees that virtually all photoelectrons that leave the cathode deliver an electrical output pulse. With its GaAsP photocathode the R10467-40 reaches a net detection efficiency of 50%. The IRF is fast and clean, and there is no background by afterpulsing as in conventional PMTs. On the negative side, the R10467-40 is not easy to use. It needs -8000 V and +400 V supply voltages, reliable overload protection, high preamplifier gain, and excellent RF shielding. bh were the first who solved these problems and completely passed to hybrid detectors in their FLIM systems [14]. A comparison of the efficiency of the different detectors can be found in the 'bh TCSPC Handbook' [2], chapter 'Detectors for TCSPC'.

A practical example is shown in Fig. 14. The image on the left was recorded with a conventional PMT (bh PMC-100-0 module), the image on the right with a GaAsP hybrid PMT (bh HPM-100-40 module). The ratio of the photon numbers is about 4.2 in favour of the GaAsP hybrid detector.

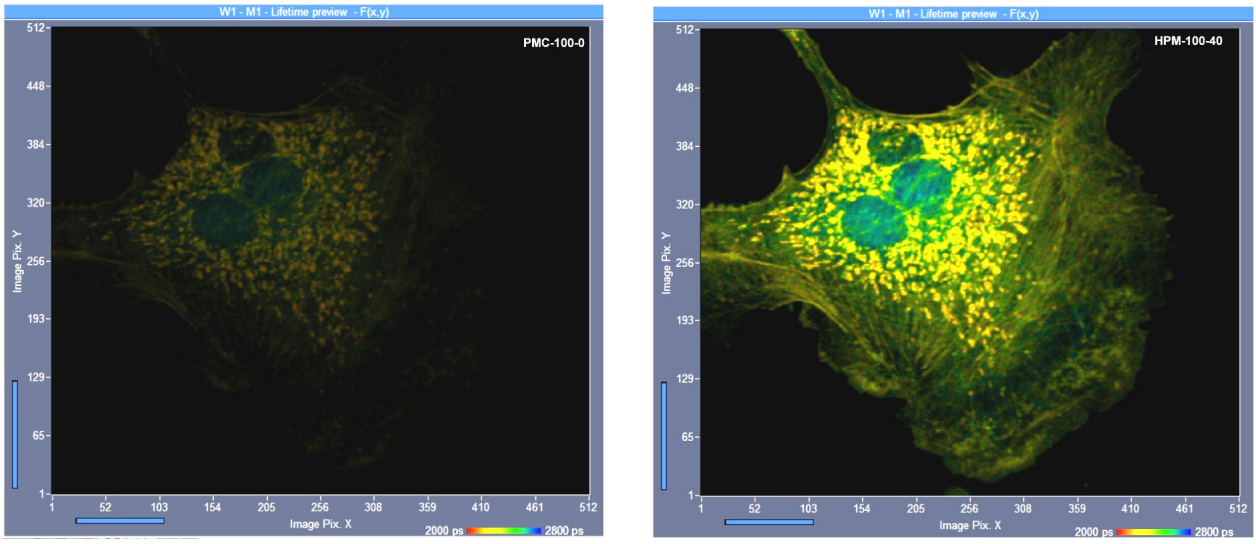

Fig. 14: FLIM image recorded with a conventional PMT (bh PMC-100-00, left) and a hybrid PMT (bh HPM-100-40, right). Identical imaging conditions, same acquisition time. The HPM-100-40 image contains 4.2 times more photons than the image taken with the conventional PMT.

Number of Pixels

The SNR of the obtained lifetimes is proportional to the number of photons per pixel. In principle, the SNR under photon-limited conditions can therefore be increased by decreasing the number of pixels. For example, a 128 x 128 pixel image needs only 1/16 of the photons of a 512 x 512 pixel image. The flaw of this approach is that it trades lifetime accuracy against spatial resolution. Unless there are other arguments for low pixel number, such as data size or scan speed, it is therefore not recommended to decrease the pixel number below 256 x 256. A far better way is to record the images with a pixel number that yields adequate spatial sampling, and use pixel binning in the data analysis [3], see section 'Data Analysis' for details. Pixel binning in the data analysis leaves the number of pixels unchanged, but runs the lifetime analysis on the sum of the decay data of the current pixel and the pixels around it. The advantage is that there is no loss in spatial resolution and no spatial undersampling, and that you

are free to select the best binning factor on the readily recorded data. An example is shown in Fig. 15. The data in the top row were recorded in a 128 x 128 pixels scan, the data in the bottom row by a 512 x 512 pixel scan. Both recordings contain the same total number of photons. Consequently, the number of photons per pixel by the 512 x 512 pixel scan is 16 times lower. However, the lower photon number was compensated by binning of pixels in the data analysis. The decay curves per binning area (bottom row) therefore contain the same number of photons as the decay curves per pixel (top row). Consequently, the lifetime histograms (shown on the right) have the same width for both recordings. However, the image from the 512 x 512 pixel scan (bottom row, left) is much sharper than the one from the 128 x 128 pixel scan (top row, left). Please see section 'Data Analysis'.

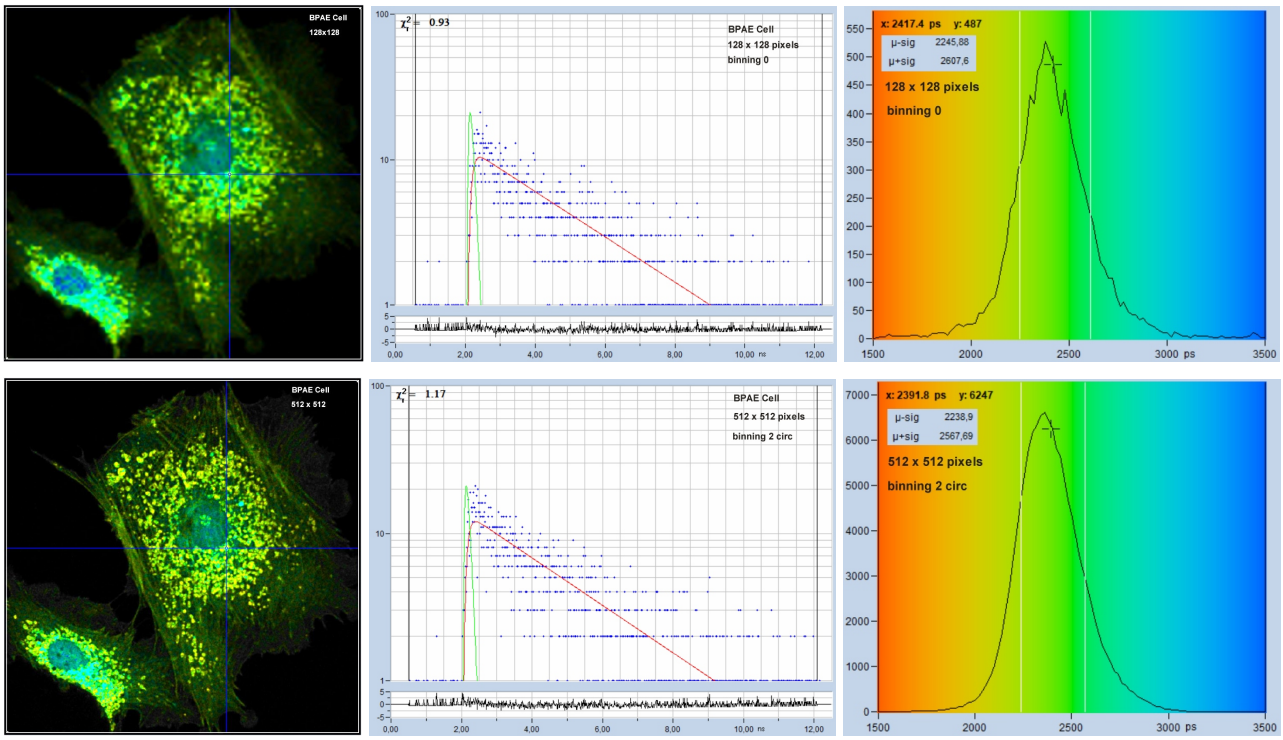

Fig. 15: FLIM data recorded with different pixel numbers. Same acquisition time, same total number of photons. Upper row 128 x 128 pixels, lower row 512 x 512 pixels. Left to right: Images, decay curves at cursor position, lifetime histogram. The 512 x 512-pixel image was analysed with pixel binning to compensate for the lower number of photons per pixel.

Maximising the Photon Efficiency

As described under 'Signal-to-Noise Ratio' a TCSPC system is able to reach the theoretical signal-to-noise ratio given by SNR = SQRT (N). This requires, however, that that every fluorescence photon seen by the detector adds its maximum possible amount of information to the result. This requires that the TCSPC timing parameters are correctly configured, that the recording of background photons is avoided, and that the photon times are determined at sufficiently high precision. These and a few other points will be considered in this section.

Observation-Time Interval

The observation time interval (the time interval over which the photon times are determined) can have an influence on the signal-to-noise ratio of the lifetime. Fig. 16 shows an example. Two images of the same sample were taken, with the same count rate and the same acquisition time. The laser repetition

rate was 50 MHz. The left image was recorded within an observation-time interval of 5 ns. The lifetime is about 2.2 ns. Therefore the fluorescence does not fully decay in the observation-time interval, see Fig. 16, second row, left. As a result, photons in the tail of the decay functions are not recorded, and the data analysis procedure can determine the lifetime from the recorded part of the decay only. The distribution of the lifetimes over the pixels is therefore broader than it would be under ideal conditions, see Fig. 16, bottom left. The situation shown in Fig. 16 is not unrealistic. Short observation time intervals can be fully appropriate for samples with extremely short lifetime. It can then happen that they are unintentionally used for long lifetimes as well, with the result that a sub-optimal photon efficiency is obtained.

The image on the right was recorded within an observation-time interval of 12 ns. Virtually all photons of the decay function are recorded, and data analysis has the entire decay function to determine the lifetime from, see second row of Fig. 16, right. As a result, the distribution of the lifetime (Fig. 16, bottom right) is narrower than for the 5-ns recording.

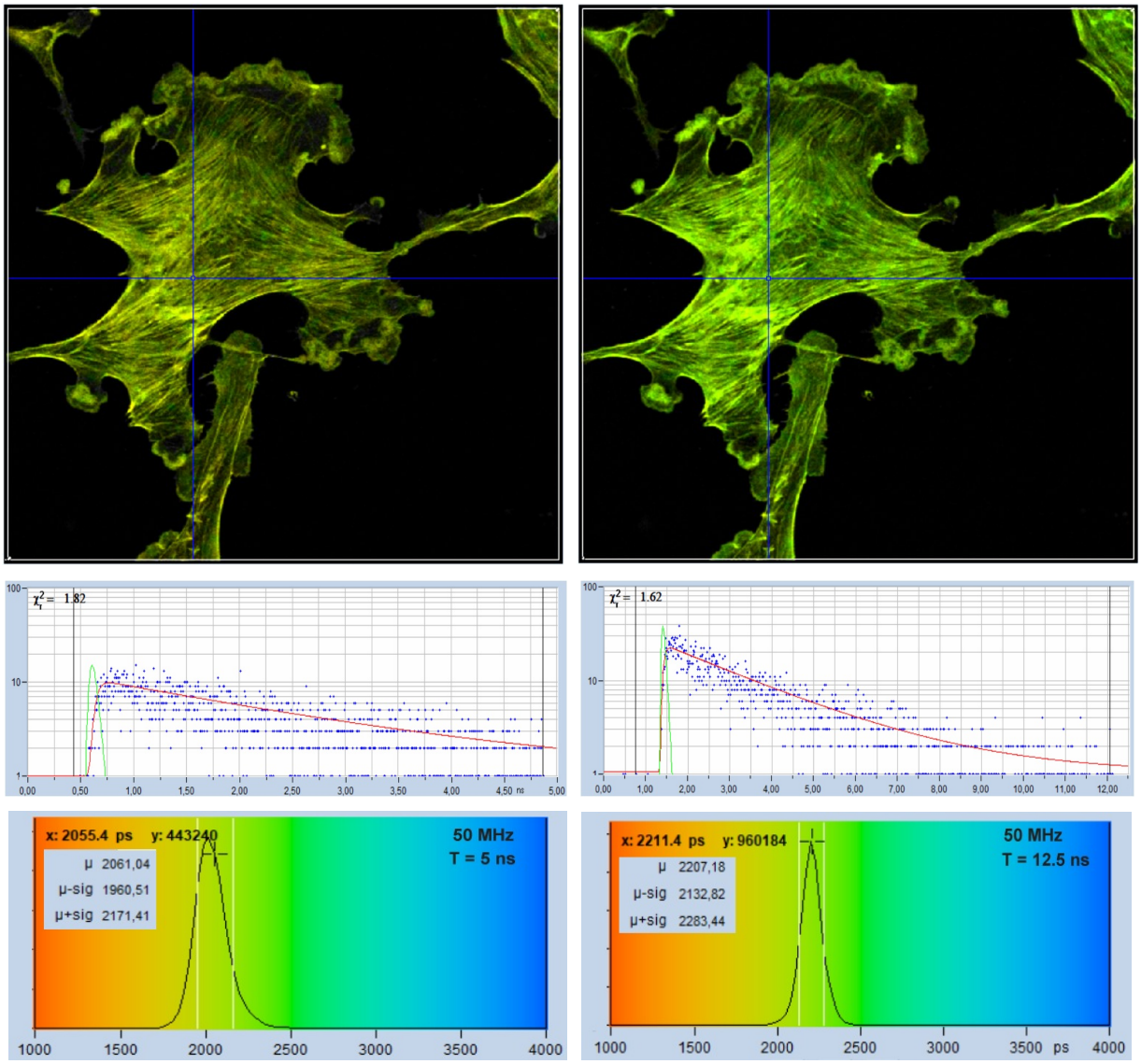

Fig. 16: Images recorded within an observation time interval of 5 ns (left) and 12 ns (right). Decay curves and histograms shown in the second and third row.

Also the way the decay curves are placed in the observation time interval can have an influence on the photon efficiency. Fig. 17 shows an example. For the left image, the decay curves have been improperly placed in the observation time window. The curves are shifted to the right, so that the far end of the decay curve is not recorded. The mistake in the parameter setup in Fig. 17, left, may look trivial and easy to correct [2]. Nevertheless, the situation is frequently encountered in TCSPC FLIM data.

In the right image, the decay data are perfectly placed in the observation time window, and the entire decay curve is recorded. Not only is there no loss of photons, a fit routine also has a larger time interval over which it can determine the lifetime. Consequently the lifetime histogram for the correctly centred decay data is visibly narrower, see Fig. 17, bottom. The standard deviation, σ_τ, is 80 ps versus 118 ps for the data on the left. This is a ratio of 1.48 in favour of the well centred decay data. A ratio of 1.48 in σ_τ may not sound very much. However, it translates into a factor of 2.18 in photon efficiency. That means the correctly configured system needs 2.18 times less photons (or 2.18 times less acquisition time!) to reach the same lifetime accuracy as the system on the left.

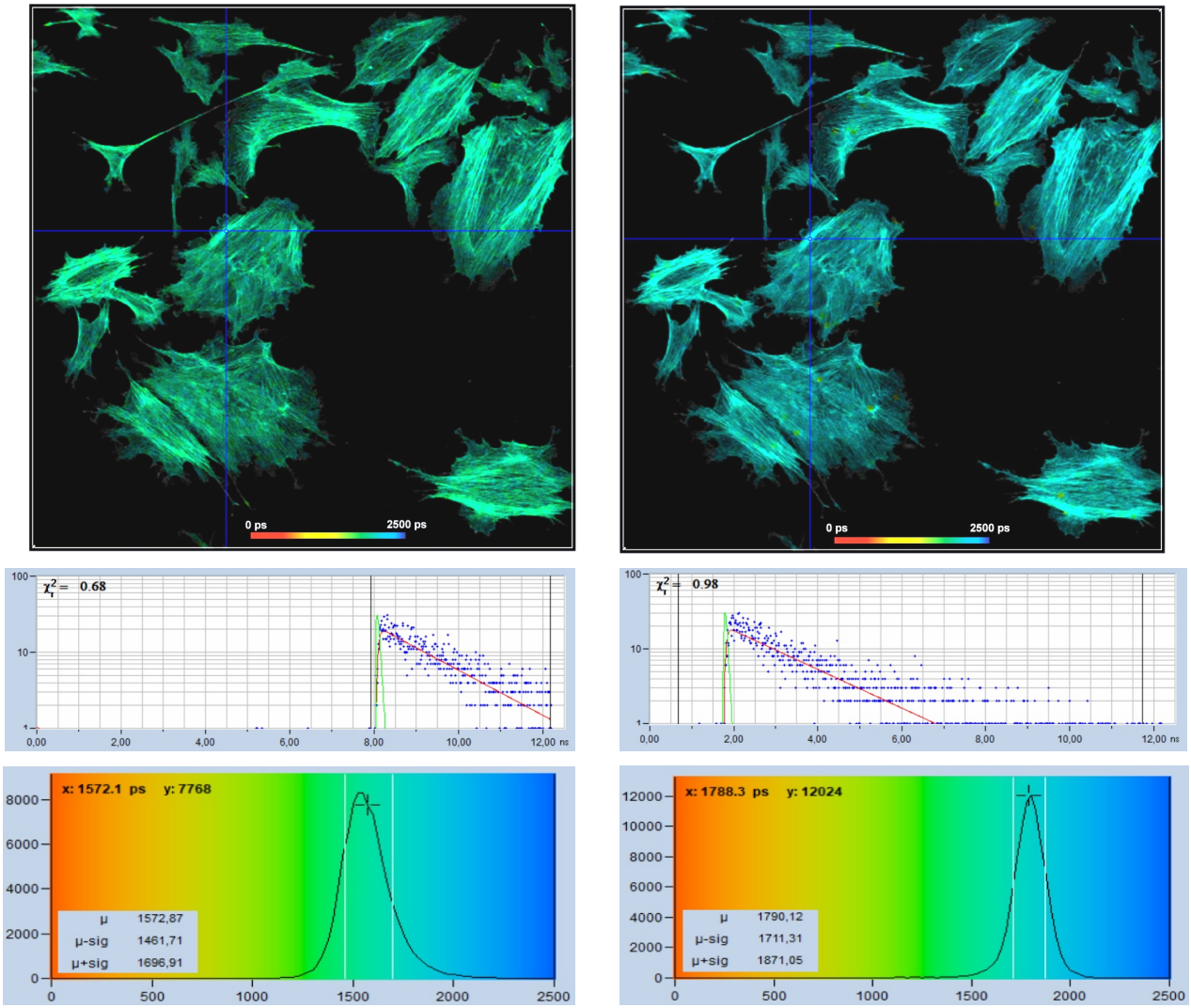

Fig. 17: Effect of sub-optimal recording of the decay curves. In the left image, the decay curves are improperly placed in the observation time window. The far end of the decay curve is not recorded. In the right image, the decay data are perfectly placed in the observation time window. The entire decay curve is recorded. The lifetime histogram for the correctly centred decay data is noticeably narrower.

A comparison of the lifetime images in Fig. 16 and Fig. 17, left and right, shows also another effect: The lifetimes in the left images are biased toward smaller values. The reason is that the fluorescence decay is not purely single exponential. The slow decay component is most prominent in the tail of the decay curve, i.e. in he missing part of the data. When the data analysis procedure fits the data with a single-exponential model it can optimise the fit for the recorded part of the decay data only. In this part the slow component is under-represented, with the result that the lifetime is determined shorter than it actually is. The situation for the first-moment technique is even worse. Since the tail of the fluorescence decay is missing the calculated moment is too small, and so is the fluorescence lifetime derived from the first moment.

Laser Repetition Rate

FLIM systems using ps diode lasers can be operated at different laser repetition rates [5, 6, 7]. Standard rates are 20 MHz, 50 MHz, and 80 MHz, but other repetition rates can be built in on demand. Multiphoton FLIM systems using Ti:Sa lasers are running at 80 MHz, and systems with femtosecond fibre lasers often use 40 MHz [17]. Which repetition rate is best? Can a fluorescence lifetime of 5 ns still be accurately determined with 80 MHz repetition rate? Should I possibly always use 80 MHz because there is more excitation power available?

Fig. 18 shows decay curves from a selected spot within the scan of a dye solution. The fluorescence lifetime is 5.6 ns. The upper curve was obtained with 50 MHz, the lower curve with 80 MHz repetition rate. The number of photons is about 20,000 and approximately the same in both curves. Both curves contain a substantial amount of 'incomplete decay' from photons that remain from the previous excitation pulse. The amount of incomplete decay is, of course, higher in the 80 MHz recording because there is less time for the fluorescence to decay. For obvious reasons, data with incomplete decay cannot be analysed by the first-moment technique. They can, however, be processed with the 'incomplete decay' models of SPCImage. Processing the images this way yields the lifetime distributions shown in Fig. 18, right.

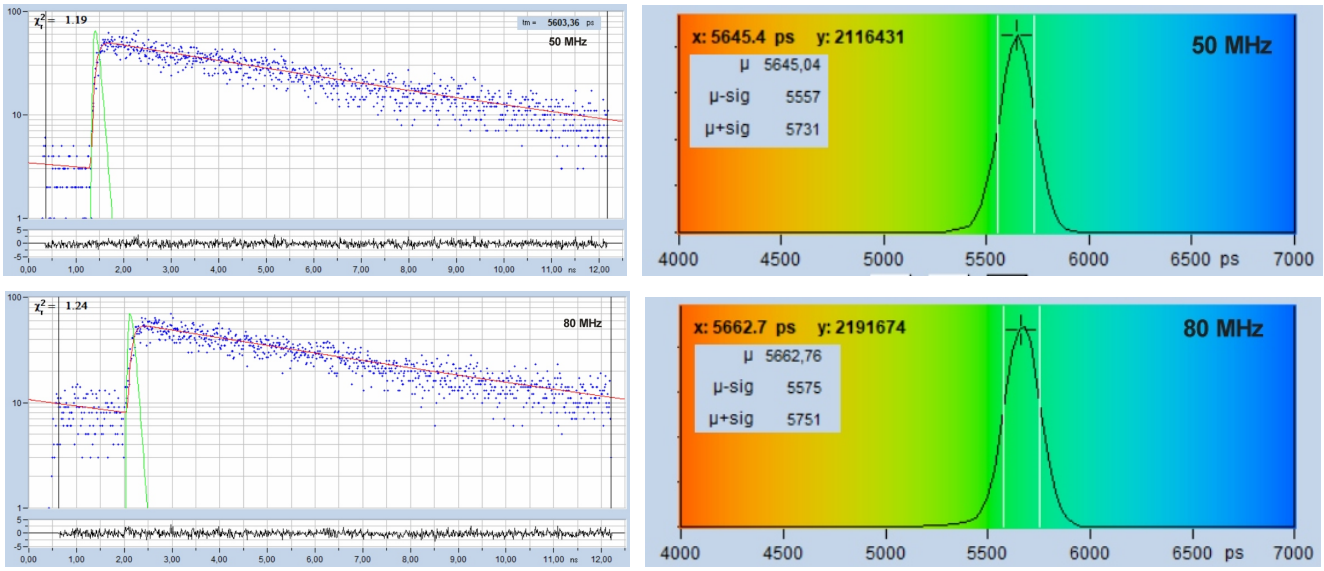

Fig. 18: Fluorescence decay functions from a dye solution, 5.6 ns fluorescence lifetime. Top: Laser repetition rate 50 MHz. Bottom: Laser repetition rate 90 MHz. Left: Decay curves. Right: Histograms of the lifetime over the pixels.

The result is a surprise: Although the 50-MHz curve looks much more 'analysis friendly' the histograms are virtually identical. Why? The reason is that the sum of a 5.6 ns decay and another 5.6-ns decay shifted by one period left is still a 5.6-ns decay. The fit procedure therefore delivers the correct lifetime with a reasonable standard deviation. The standard deviation is larger that the ideal value for 20,000 photons but it is the same for both recordings. The loss against an ideal recording comes from the fact that the recording time interval does not cover the entire decay, not from the fact that incomplete decay is present. This is supported by Fig. 19. It shows a recording at 50 MHz but within an observation-time-interval of 20 ns. The lifetime distribution obtained from these data is noticeable narrower.

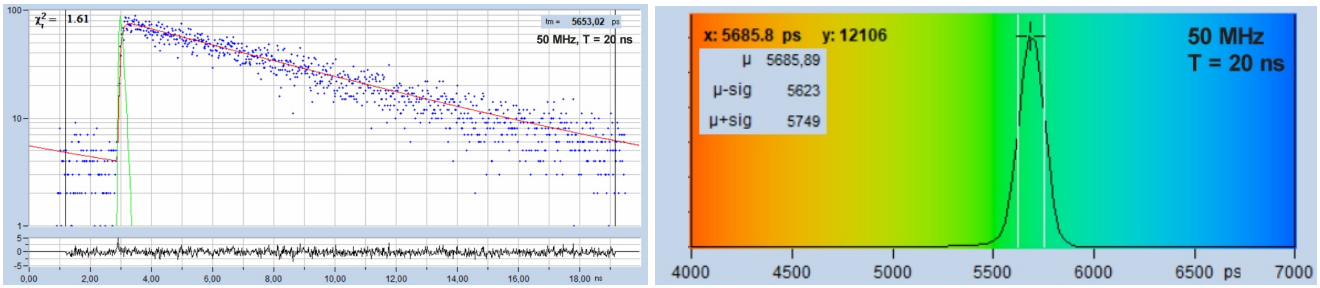

Fig. 19: Fluorescence decay of 5.6 ns, recorded with 50 MHz repetition rate and within a recording time interval of 20 ns.

The conclusion is: If possible, use a recording time window that covers as much as possible of the fluorescence decay. If you can't do so because the laser pulse period is too short, don't worry. Data analysis will takes care of the incomplete decay and extract the best lifetime information possible.

Counting Background

Counting background is not only the most common flaw in FLIM data, it is also the most devastating one. Fortunately, it is also the one that is easiest to avoid. In most cases, the background just comes from pickup of daylight. Most vulnerable are multiphoton systems with non-descanned detection. These systems have no pinhole that rejects light from outside the excited spot. They are designed to detect photons that are scattered on the way out of the sample. To do so, they collect light from a large area of the sample surface. The side effect is that they are also sensitive to ambient light. Keeping off daylight from the detection system is therefore imperative.

Fig. 20 shows what happens if the decay data are overlaid by background counts. The fluorescence photons (a) have an average arrival time $\langle t \rangle = \tau$, and a timing noise of $\sigma_t = \tau$. Could we build up a photon distribution of the fluorescence photons alone, it would represent the true fluorescence decay curve (a, right), an deliver the fluorescence lifetime with a standard deviation of $\sigma_\tau = \tau$ / SQRT (N), i.e. with a photon efficiency of one.

The background photons (b) spread evenly over the entire observation time window, T. Their average arrival time is T/2, and their timing noise is $\sigma_{tbkg} = 0.28$ T (see Fig. 24, page 25).

The recording process makes no difference between fluorescence and background photons. The detected signal (c) is therefore the sum of the fluorescence decay and the background. This causes two unpleasant effects. First, the average arrival time is no longer the fluorescence decay time, τ. Instead, it is a photon-number weighted average of the lifetime, τ, and the average arrival time of the background photons, T/2. The data therefore cannot be analysed by the first-moment technique, or by any other technique based on moments.

Second, the effective timing noise is a weighted sum of the timing noise of the fluorescence photons, $\sigma_t = \tau$, and the timing noise of the background, $\sigma_{tbkd} = 0.28$ T. In most instances 0.28 T is larger than τ. It thus has a large influence of the net standard deviation, $\sigma_{\tau meas}$ of the measured lifetime. An exact calculation of $\sigma_{\tau meas}$ and thus of the photon efficiency is difficult and delivers results which cannot easily be interpreted. Nevertheless, the considerations above show that counting background has a large effect on the detected lifetimes.

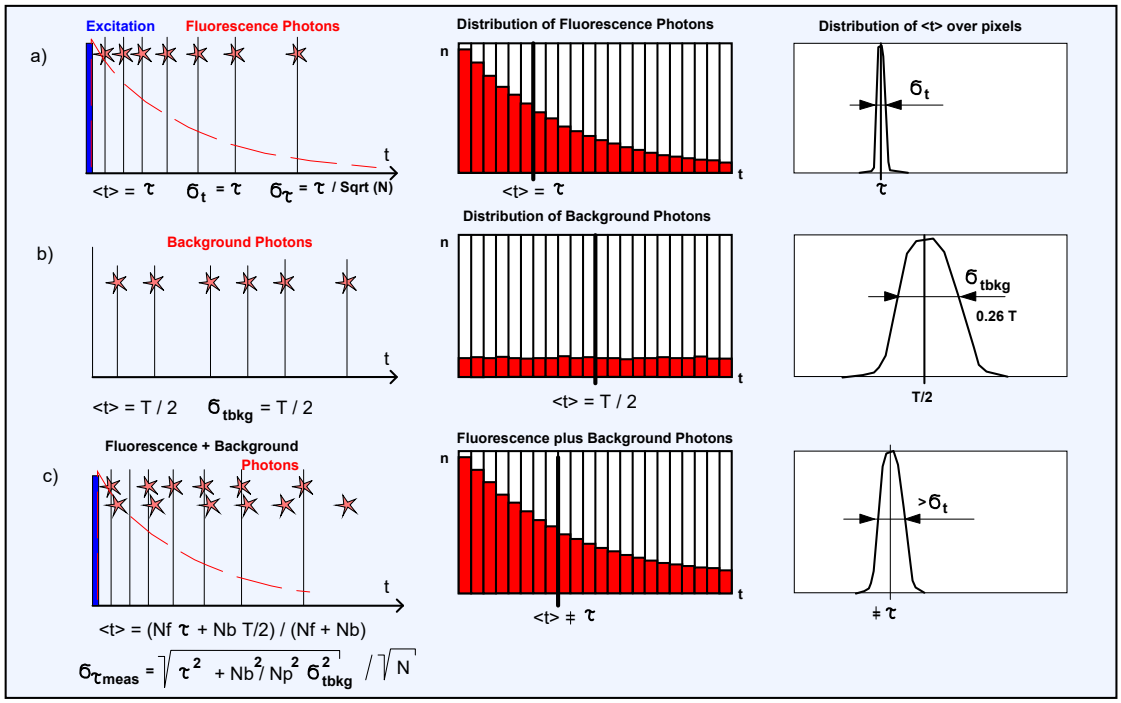

Fig. 20: Effect of counting background on the photon times

A practical example is shown in Fig. 21. FLIM images from the same sample were recorded with background (left) and without (right). In the left image, the background in each pixel is about 900 counts (sum over all time channels), in the right image it is close to zero. The number of fluorescence photons in the brightest pixels is about 4000. The background therefore visibly impairs the contrast of the image, see Fig. 21, left. The loss in contrast is no so bad, however, to obscure the image entirely. The right image is free of background and thus provides maximum contrast.

The decay curves in a selected spot are shown in the second row. The decay curve from the left image contains background counts, the decay curve from the right image does not. The background seems moderate and does not look like a real problem. Nevertheless, the effect on the lifetime accuracy is enormous. This can be seen in the third row of Fig. 21. It shows, for each of the recordings, a phasor plot, and a histogram of the lifetime calculated by first moments. It can easily be seen that the histogram and the phasor plot for the left data set are not only entirely off but also extremely widened. The reason is not only that the background adds timing noise to the photon data but also that the background adds an offset to the moments. Since the ratio of fluorescence and background changes with the brightness of the pixels the lifetime values get extremely smeared out.

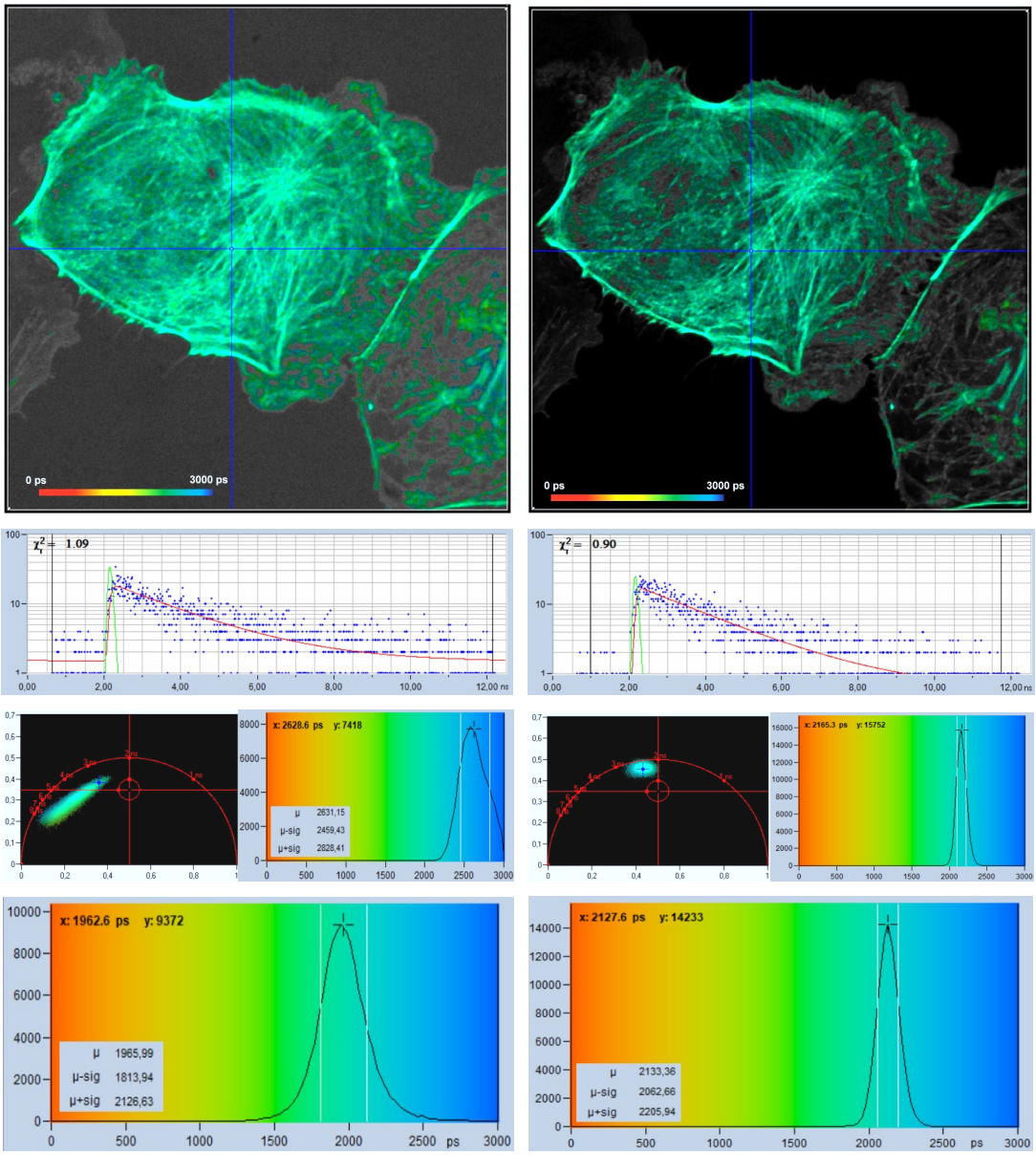

Fig. 21: Effect of counting background on FLIM accuracy. Left: FLIM data with background counts. Right: Background-free recording. Upper row: Images. Second row: Decay data in selected spot. Third row: Phasor plots and lifetime histograms of M1 analysis. Lower row: Lifetime histograms from MLE analysis.

The bottom row of Fig. 21 shows histograms of the lifetimes obtained by MLE analysis. In terms of lifetime shift the fit procedure does better than moment analysis. Nevertheless, the lifetime is by about 170 ps off, and the histogram is by a factor of two wider than that of the background-free recording on the right. A factor of two in lifetime standard deviation translates into a factor of four in photon efficiency!

Number of Time Channels

In contrast to widespread opinion, the number of time channels in the decay curves has no direct influence on the signal-to-noise ratio. It does not appear in the equation of the SNR (section 'Signal-to-Noise Ratio') derived for first-moment analysis, and data analysis by fit routines does not care whether FLIM data have half the number of photons in twice the number of time channels or vice versa. Only

the total number of photons in the decay curve matters. An experimental verification is given in Fig. 22. It shows a sample stained with Alexa 488. At the detection wavelength used, the lifetime is almost uniform over the entire scan area. The data in the first row were recorded with 64 time channels, the data in the second row with 1024. The total number of photons in the images is virtually the same. As expected, the lifetime histograms (first and second row, right) are almost identical.

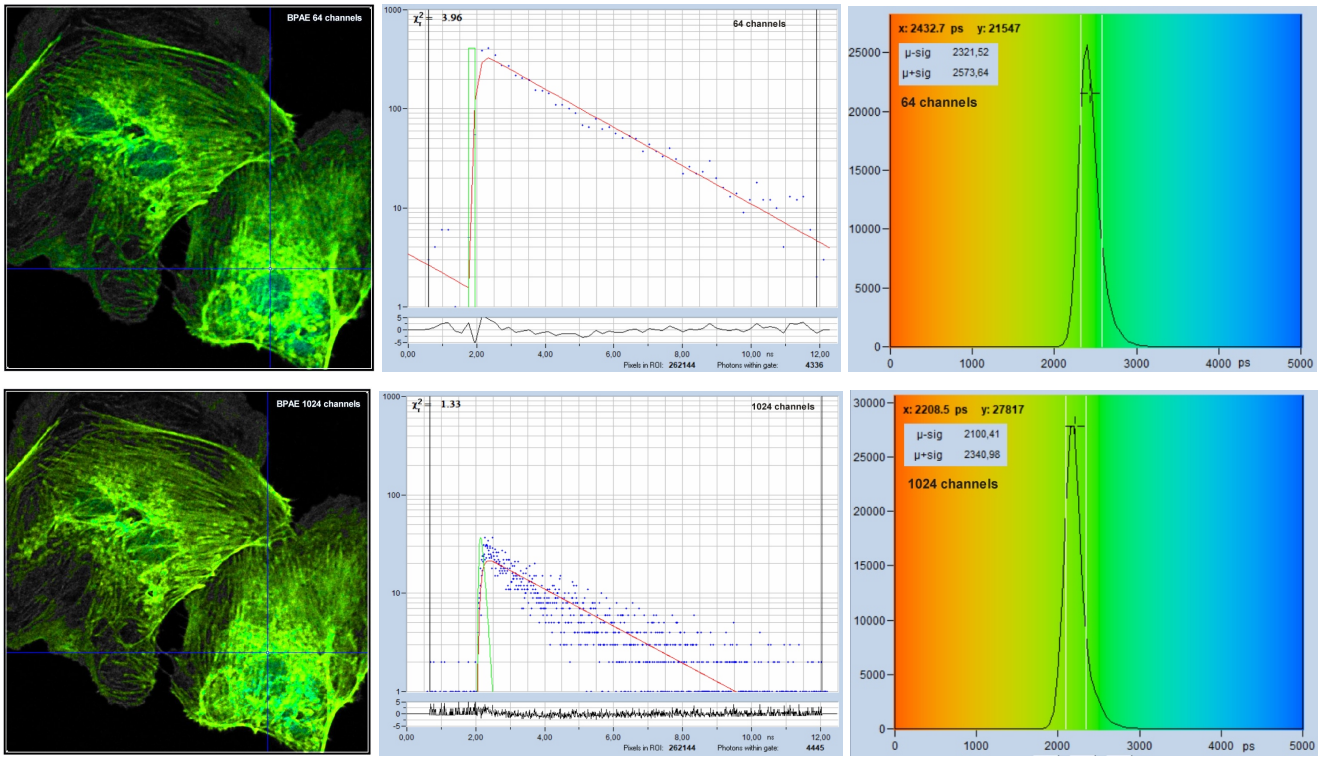

Fig. 22: Recording with different number of time channels, same total number of photons. Upper row: 64 time channels. Lower row: 1024 time channels. Left to right: Image, decay curve at cursor position with single-exponential fit, histogram of lifetime over the pixels. In contrary to widespread opinion the higher number of photons per time channel in the 64-channel recording does not yield to a higher lifetime accuracy.

The fact that the SNR of the lifetime is independent of the number of time channels does not mean that arbitrary small numbers of time channels and arbitrary large time-channel widths can be used. Detecting in just two or four time channels massively decreases the photon efficiency [1, 13, 19]. However, degradation of the SNR already starts when the time channel width is on the order of the IRF width. It is then not clear where in the first time channel the IRF is located, and where the rise of the fluorescence pulse starts. This adds uncertainty to the lifetime determination. As a rule of thumb, both the IRF and the fastest decay component should be sampled with no less than 5 to 10 time channels. That means, for an HPM-100-40 detector (IRF width 120 ps) and fast decay components down to 100 ps the time channel width should be about 10 ps. For an observation-time interval of 10 ns the number of time channels should then be 1024. For an HPM-100-06 (IRF width <20 ps) it is not ridiculous to increase the number of time channels to 4096, i.e. decrease the time channel width to 3 ps. Even narrower time channels may be appropriate if ultra-fast decay components are to be detected.

Influence of the IRF

What happens if the IRF of the FLIM system has non-zero width? The effect of the IRF can, again, be estimated by looking at the photon arrival times. Let's assume that we have recorded or otherwise determined the IRF of the FLIM system. We can then define a 'centroid' of the IRF by averaging the photon times from the IRF measurement, $<t_{irf}>$. As shown already in Fig. 6, page 9, the fluorescence decay time, τ, is obtained by simply subtracting $<t_{irf}>$ from the average photon times $<t>$, see Fig. 23, left.

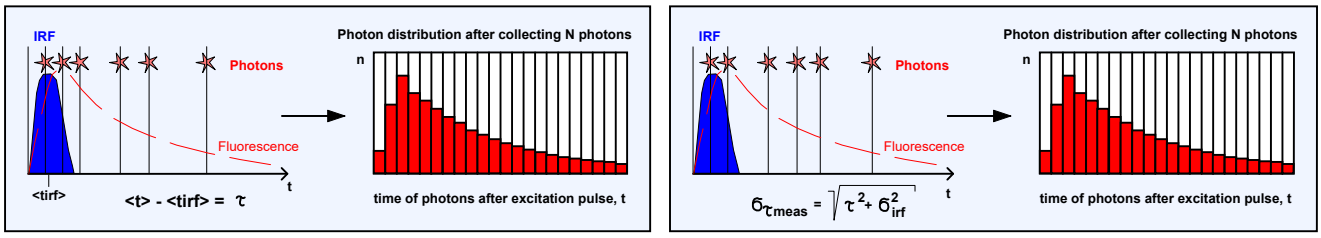

Fig. 23: Standard deviation of lifetime measurement in a system with no-zero IRF width. Left: The lifetime is the average arrival time, t, of the photons minus the time of the IRF centroid, $<t_{irf}>$. Right: The standard deviation of the measured lifetime, τ_{meas}, contains a contribution from the IRF, σ_{irf}.

What is the standard deviation of the lifetime obtained this way? One could presume that the standard deviation is still τ / SQRT(N): The centroid of the IRF is accurately known, and subtracting it does not change the standard deviation of t. This is wrong. It is wrong because the photon times themselves now contain an uncertainty from the IRF. Every fluorescence photon has its timing reference at a different time in the IRF. It may have been excited at a different time in the laser pulse, or it has spent a different time transiting the detector. This adds an uncertainty to the photon times, t, and adds a contribution of the IRF, σ_{irf} , to the standard deviation, $\sigma_t = \tau$, of the ideal photon times.

The standard deviation of the measured photon times σ_{tmeas} is therefore larger than τ, and the standard deviation of the measured lifetime, $\sigma_{\tau meas}$, is larger than τ / SQRT(N). It can be estimated by quadratically adding the standard deviation of the photons in the ideal fluorescence decay, τ, and the uncertainty from the IRF, σ_{irf} :

$$\sigma_{\tau meas} = \text{SQRT}\,(\tau^2 + \sigma^2_{irf}) \,/\, \text{SQRT}\,(N) \quad \text{or}$$

$$\text{SNR}_{\tau meas} = \text{SQRT}\,(N) \cdot \text{SQRT}\left(\frac{1}{(1 + \sigma^2_{irf} / \tau^2)}\right)$$

σ_{irf} is also known as 'RMS Timing Jitter' or - a bit misleading - 'IRF width RMS'. For IRF shapes encountered in practice it is about 0.43 to 0.87 of the full-width at half maximum (FWHM) of the IRF. The RMS versus the FWHM values for a few typical IRF shapes are given in Fig. 24. For a Gaussian IRF the RMS timing jitter is 0.43 FWHM. For asymmetrical functions it is larger than this. IRFs with slow tails or with bumps add more timing noise to the decay data, and should, if possible, be avoided. Please note that tails and bumps can also originate from picosecond diode lasers operated at excessively high power. The accuracy loss by the unfavourable IRF shape can in fact outweigh the gain from the increased number of photons.

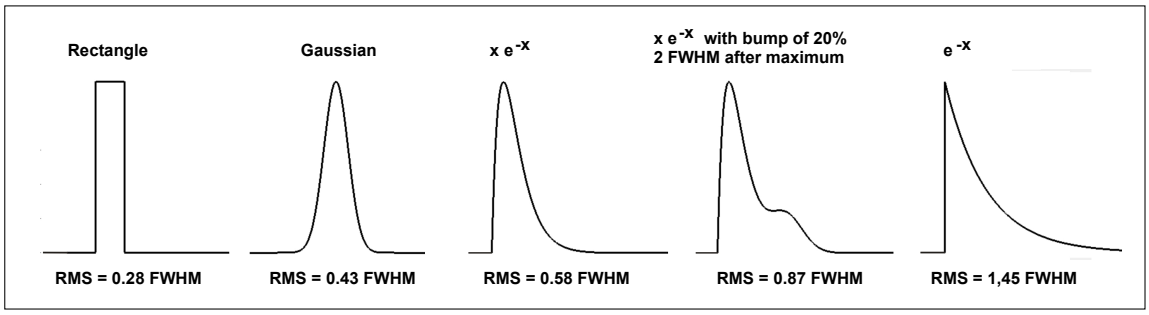

Fig. 24: RMS values for a number of typical IRF shapes. Left to right: Rectangle, Gaussian, $x \cdot e^{-x}$, $x \cdot e^{-x}$ with a bump 2 FWHM after the maximum, exponential function e^{-x}. Functions normalised to same FWHM, RMS values given in fractions of the FWHM.

There are two conclusions from this result. The first one is that, not surprisingly, the SNR still scales with the square root of N. The second one is that a massive decrease in SNR occurs only when the RMS of the IRF width becomes larger than about 50 to 100% of the fluorescence lifetime.

The slow degradation of the lifetime accuracy with increasing IRF width is surprising. It has led to the misconception that the IRF width of a FLIM system is not important: The fluorescence lifetimes of typical fluorophores are in the range of a few nanoseconds. Therefore an IRF width of 500 ps to 1 ns (RMS) should be sufficient, if only the IRF is exactly known. However, this contradicts any practical experience. Where is the mistake?

The fluorescence decay functions in FLIM are not single-exponential. More than that, the desired information often is in the composition of the decay function rather than in the net 'lifetime'. In that case, the IRF must be faster than the fastest decay component. Major decay components in FRET measurements and in autofluorescence measurements range down to about 300 ps and 100 ps, respectively [2]. The HPM-100-40 detector is a good match to these applications. Lifetimes down to the 10 ps range are encountered in mushroom spores [15], in human hair, and in lesions of mammalian skin. These measurements require an even faster detector. Examples will be shown in section 'Multi-Exponential Decay Functions'.

Multi-Exponential Decay Functions

A single-exponential approximation of the fluorescence decay and the measurement of its apparent lifetime may be sufficient when FLIM is just used as a contrast technique in laser scanning microscopy. However, the real applications of FLIM are in molecular imaging. Fluorophores - either endogenous or exogenous ones - change their fluorescence lifetimes depending on their molecular environment. This may be binding to proteins, protein configuration, interaction of proteins with others, effects of the metabolic state of cells or tissues, or the concentration of ions involved in the function of the cells. In these applications the task is not to distinguish different fluorophores but to distinguish fractions of the *same* fluorophore in different molecular environment and quantify them by their relative concentrations [1, 4, 18]. In most cases this requires recording of multi-exponential decay functions and splitting them into different decay components. Multi-exponential decay recording and multi-exponential decay analysis are therefore standard in FLIM of biological systems. A few examples are shown in Fig. 25 and Fig. 26. More examples of multi-exponential FLIM measurements are shown in Fig. 31, Fig. 32, and Fig. 41.

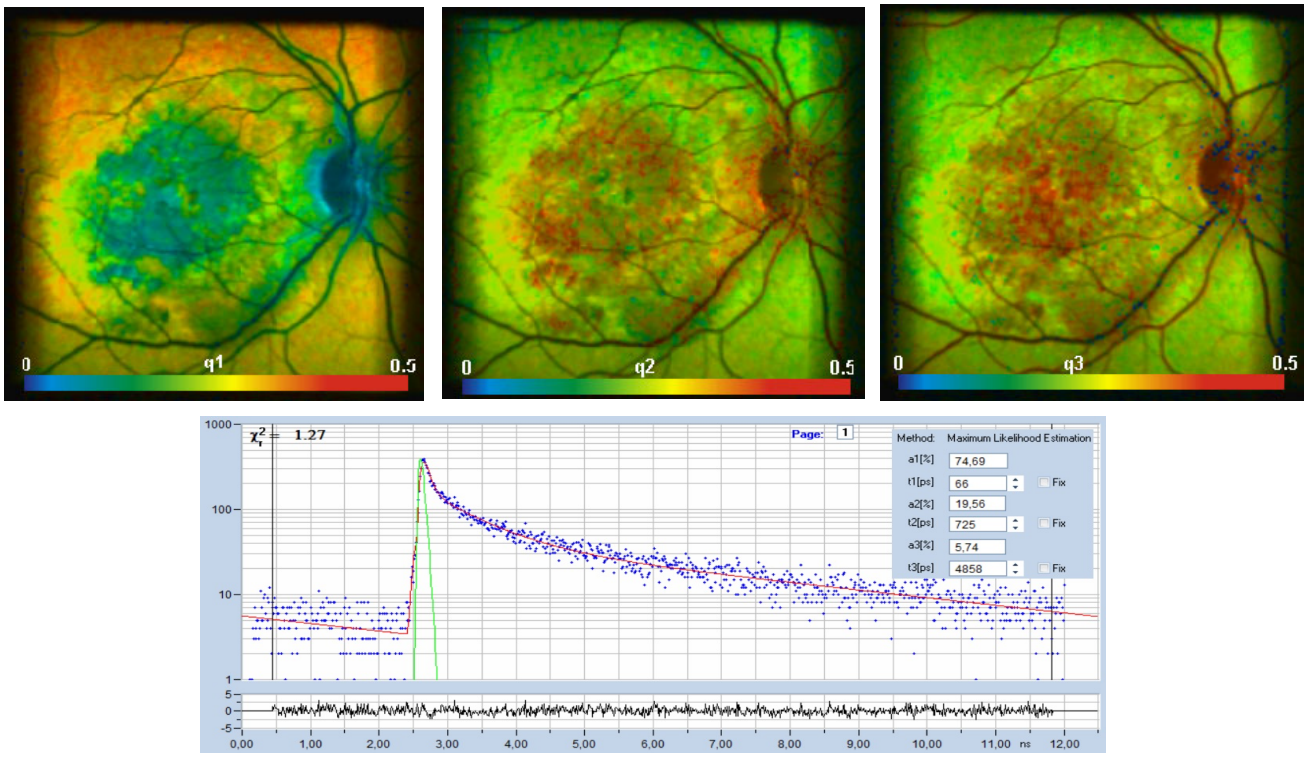

Fig. 25: Top: FLIM Images of the human retina, recorded in vivo. Intensity contribution of the fast, medium, and slow decay component. Bottom: Decay curve in selected spot of the image. Data courtesy of Dietrich Schweitzer and Martin Hammer, University of Jena.

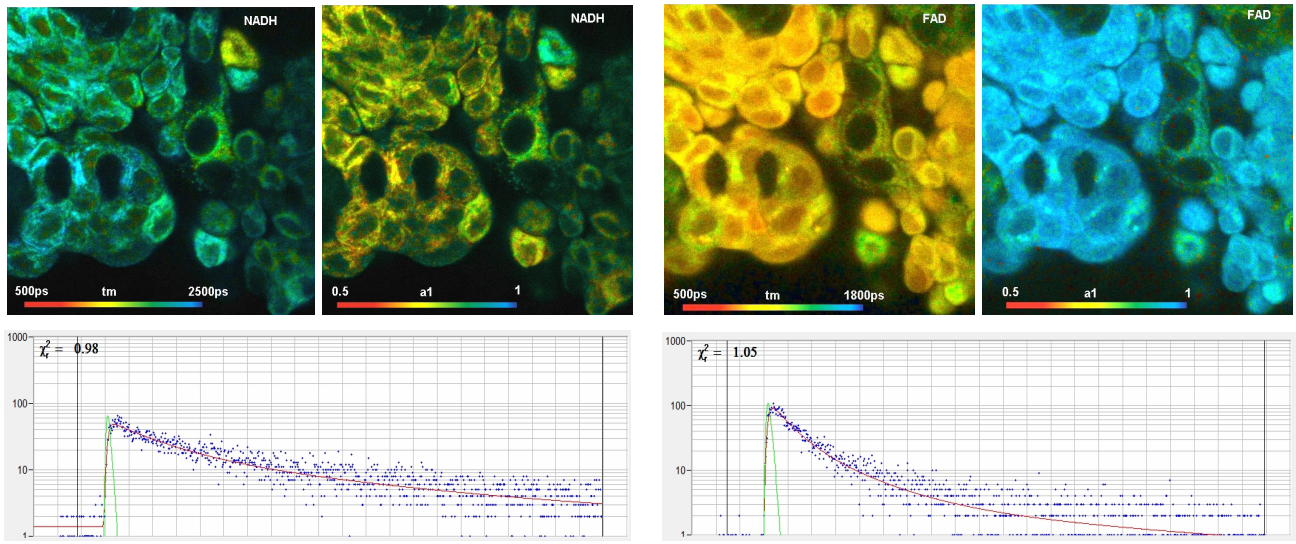

Fig. 26: Metabolic imaging by FLIM of NADH (left) and FAD (right). Images of the amplitude-weighted lifetime, tm, of double-exponential decay, and of the amplitude of the fast decay component, a1. Bottom: Decay functions in selected spot of the NADH and the FAD image.

Extracting individual decay components from a multi-exponential decay analysis requires more photons than a single-exponential fit or first-moment analysis [20]. Therefore, detection efficiency and photon efficiency are the crucial parameters. Time resolution is important as well - the requirements to the IRF width are given by the lifetime of the fastest decay component, not by the apparent lifetime of the net decay function.

What also matters is the shape of the decay functions. The more they differ from a single-exponential decay the better. Decay components that have nearly the same lifetime are hard or impossible to split [20], and decay components with low amplitudes are difficult to extract. Three examples are shown in Fig. 27. The function shown left contains 82 % of 445 ns on the background of 2.4 ns. It is easy to resolve. The function in the middle is more difficult. The amplitude of the fast component is only 24 %, and the lifetime is almost 900 ps, compared to 2.5 ns of the slow one. The net decay function is much closer to single-exponential than the one on the left. The decay profile on the right is visually indistinguishable from a single-exponential decay. It contains 35 % of 3 ns and 65 % of 4.5 ns. With the number of photons typically available in FLIM it cannot be resolved on a pixel-by-pixel basis.

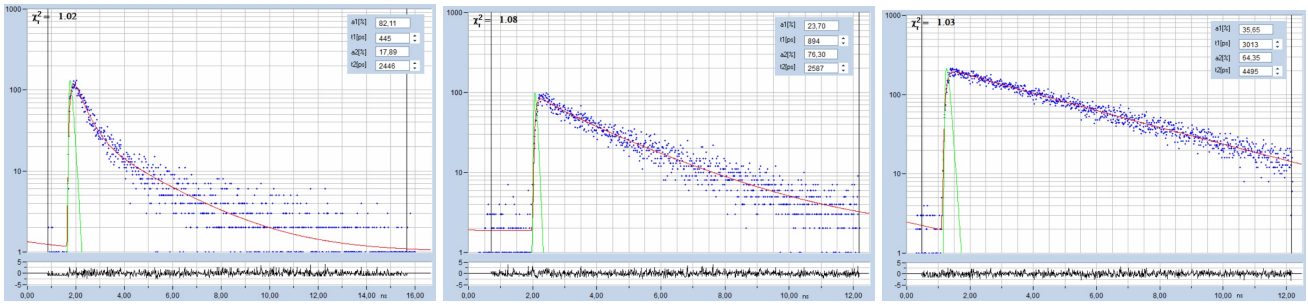

Fig. 27: Double-exponential decay functions. The function on the left is easy to resolve, the function in the middle is difficult, and the one on the right is virtually impossible to resolve in FLIM data.

Situations as the one shown in Fig. 27, right, should, if possible, be avoided already in the experiment planning. An example are FRET experiments: FRET pairs with large donor-acceptor overlap and FRET constructs with short donor-acceptor distance and large fractions of interacting donor deliver donor decay functions with a large amplitude and a short lifetime of the fast component. This make it easier to resolve the decay profile, and thus separate interacting and non-interacting donor fractions.

In some cases the results can be massively improved if the signals are spectrally separated. The number of decay components is then reduced, and the analysis becomes easier. Spectral separation can be obtained both on the excitation and on the detection side. An example is metabolic imaging by NADH / FAD FLIM. When both fluorophores are excited at the same wavelength (as it is often attempted) and only observed through different emission filters the situation can be virtually hopeless. However, by multiplexed excitation and detection in the right wavelength intervals the signals can be well separated [18]. Experiment planning, both in terms of sample design and FLIM configuration, therefore has a large influence on the quality of the results.

Fig. 28 and Fig. 29 give examples of multi-exponential decay measurement. Fig. 28 shows FLIM data of an NADH solution. A solution was used to obtain a homogeneous lifetime distribution over the entire scan area. The parameter histograms over the pixels are then determined by the photon noise, not by lifetime variation over the scan area. The data were recorded with two-photon excitation at 785 nm, images were scanned with 512 x 512 pixels, 1024 time channels. From top to bottom, Fig. 28 shows data recorded with a H7422-40 PMT detector, and by HPM-100-40 and HPM-100-06 hybrid detectors. The IRF widths are 250 ps, 110 ps, and 18 ps, respectively. From left to right, the figure shows a decay curve in an arbitrary selected spot, a histogram of the lifetime of the fast component, t1, a histogram of the second fast component, t2, and a histogram of the slow component, t3.

It can clearly be seen that the lifetime histograms become narrower with decreasing IRF width. Interestingly, this is not only the case for the fast component but also for the medium and slow component. The best result is obtained with the HPM-100-06, i.e. with an IRF width of 18 ps. Decay data recorded with an IRF this fast are virtually unimpaired by IRF-induced timing jitter. The

histograms of t1, t2, and t3 are by a factor of 1.4 narrower than for the H7422. That means the photon efficiency for the fast detector is 2 times higher.

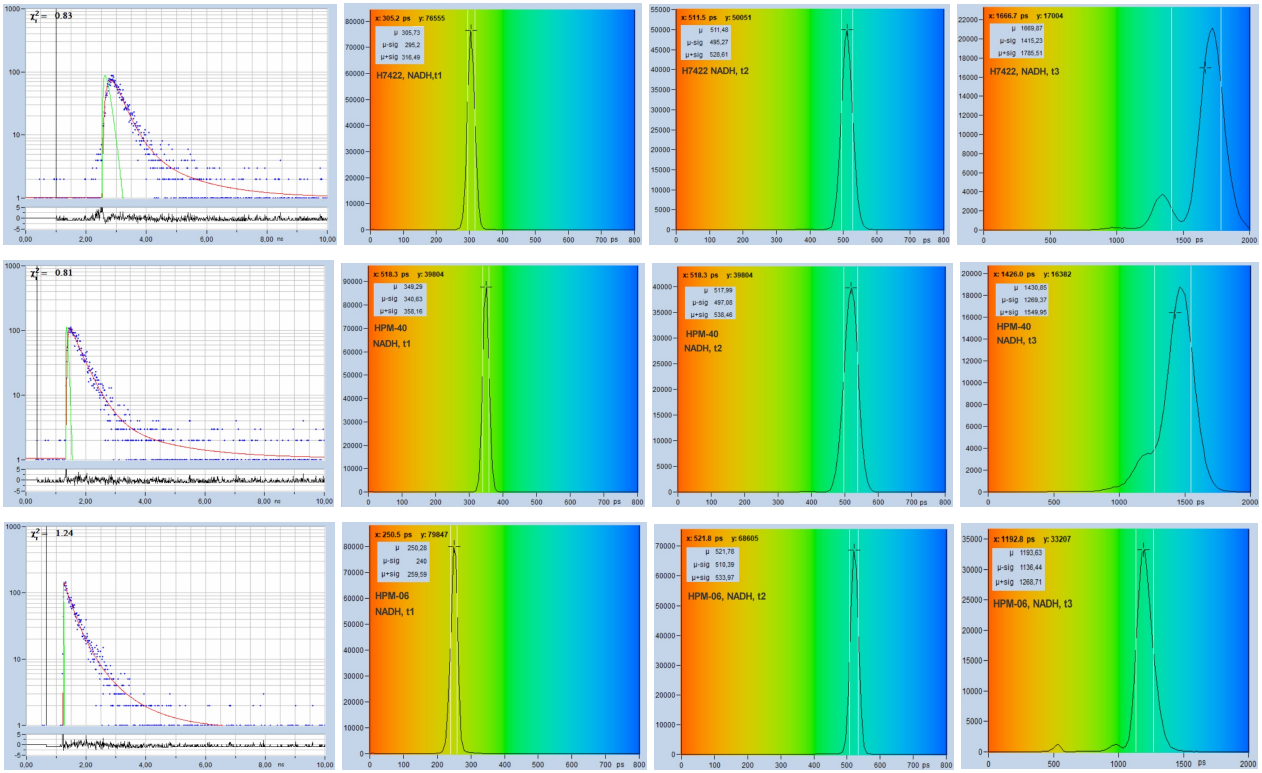

Fig. 28: NADH solution, data recorded with different detectors. Upper row: H7422-40 detector, IRF width 250 ps. Second row: HPM-100-40, IRF width 110 ps. Lower row: HPM-100-06, IRF width 18 ps. Left to right: Decay curve in arbitrary selected spot, histogram of the fast component, t1, histogram of the second fast component, t2, histogram of the slow component, t3. Two photon excitation, non-descanned detection, images 512 x512 pixels, 1024 time channels, about 5000 photons in binning area.

Fig. 29 gives an example of the detection of an ultra-fast decay component with sub-25ps lifetime. Such fast components are more frequent than commonly believed. We find them routinely in human hair, mushroom spores and in nevi of mammalian skin. A fast component exists also in the fluorescence decay of Flavine Adenine Dinucleotide, FAD, a natural fluorophore that is present in every cell. FAD is important because its fluorescence decay function contains information on the metabolic state of the cell.

Fig. 29 shows FLIM images of an FAD solution. Left to right, the figure shows images of the fast decay component, t1, of a triple-exponential fit, a decay curve, and a histogram of t1. The data in the upper row were recorded with an HPM-100-40 detector, the data in the lower row with an HPM-100-06. Visually, the decay curve recorded with the HPM-100-40 (IRF 110 ps FWHM) shows no trace of a fast component. However, careful data analysis extracts a component with a lifetime on the order of 20 ps. It would elude attention unless it is explicitly searched for. The histogram of the t1 values over the entire image is shown on the right.

The lower row of Fig. 29 shows data recorded with an HPM-100-06 (IRF width 18 ps FWHM). The decay curve convincingly shows that the fast component is indeed present. Data analysis in the selected spot of the image delivers a lifetime, t1, of 16.5 ps for the fastest component (the other two components are 2.2 ns and 3.2 ns). The histogram shows that the most frequent t1 value is about 16 ps.

As expected from the fast IRF, the histogram is by almost a factor of 2 narrower than that for the HPM-100-40 data.

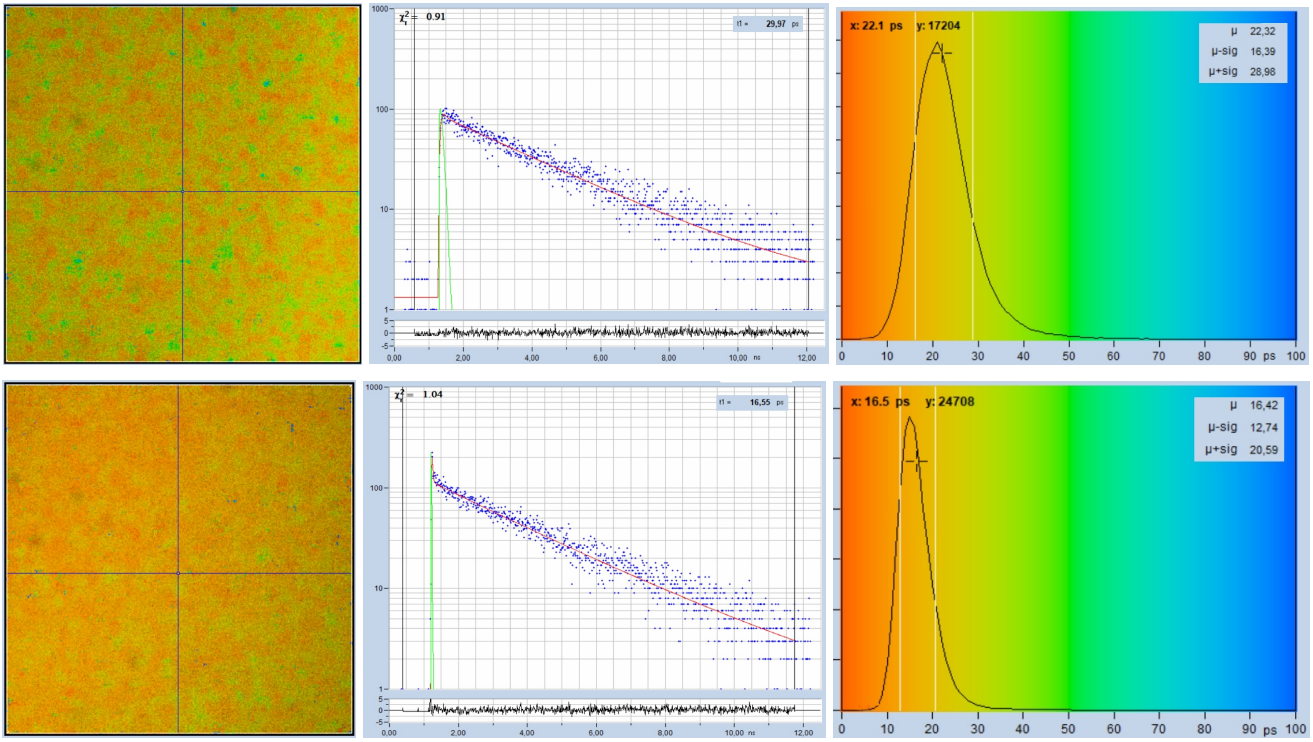

Fig. 29: Fluorescence of an FAD solution. Left to right: Image of the fast decay component, t1, of triple-exponential analysis, decay curve, histogram of t1. Upper row: Recorded with HPM-100-40 detector, IRF width 110 ps FWHM. Lower row: Detected with HPM-100-06, IRF width 18 ps FWHM.

IRF Width versus Detection Efficiency

It should be noted that there is a potential conflict between the IRF width and the efficiency of the detector. The fast detectors have conventional bialkali photocathodes. They are thus about 4 times less sensitive than the GaAsP detectors. It is not a priori clear whether faster IRF or higher sensitivity is more important. Certainly, for resolving ultra-fast decay components there is no way around the fast IRF. It is a big difference whether you actually *see* the fast component or have to squeeze it out from the data by deconvolution. We also found that double- and triple-exponential decay analysis of NADH and FAD data is more reliable with a sub-20-ps IRF [2, 16]. This can also be seen in Fig. 28, bottom. In practice the decision for one detector or the other depends on the photostability of the sample. If the sample remains stable under four times the excitation power or during four times the acquisition time the fast detector is the right one. If it doesn't the GaAsP detector must be used.

High-Count-Rate Artefacts

The FLIM literature is full of incorrect statements on the 'Pile-Up' effect and its influence of FLIM results. Pile-Up is the detection of a second photon in the same laser pulse period with a the first one. As a result, the second photon is lost, and the recorded decay profile gets distorted. Truth is, that the influence of pile-up on FLIM results is vastly over-estimated. A mathematical analysis of the pile-up effect is described in [1] and [2]. It turns out that FLIM can be recorded at count rates up to 10% of the

laser pulse repetition rate without noticeable error in the recorded decay data. For typical pulse repetition rates of 50 to 80 MHz this is higher than a typical FLIM sample can deliver.

Pile-up should not be confused with 'Counting Loss'. Counting loss is the loss of photons within the dead time (the signal processing time) of the TCSPC module after the detection of a previous photon. Counting loss has no immediate influence on the decay data but has an influence on the recorded intensities. With increasing count rate the intensity characteristics becomes nonlinear, flattens and, finally, saturates. As a result, the images are losing contrast an get an ugly 'flat' appearance. For the SPC-series FLIM modules this becomes noticeable at detector (CFD) count rates of 5 to 10 MHz.

The effect of counting loss can be avoided by the 'Lifetime-Intensity' mode of the bh TCSPC FLIM modules [10]. The mode is using a fast counter in parallel with the TCSPC timing electronics. The SPCM data acquisition software builds up FLIM images by using pixel intensities from the parallel counter and pixel decay data from the timing electronics. A comparison is shown in Fig. 30. If you see a loss in contrast as in Fig. 30, left, pass to the INT-FLIM mode. Details are described in [10].

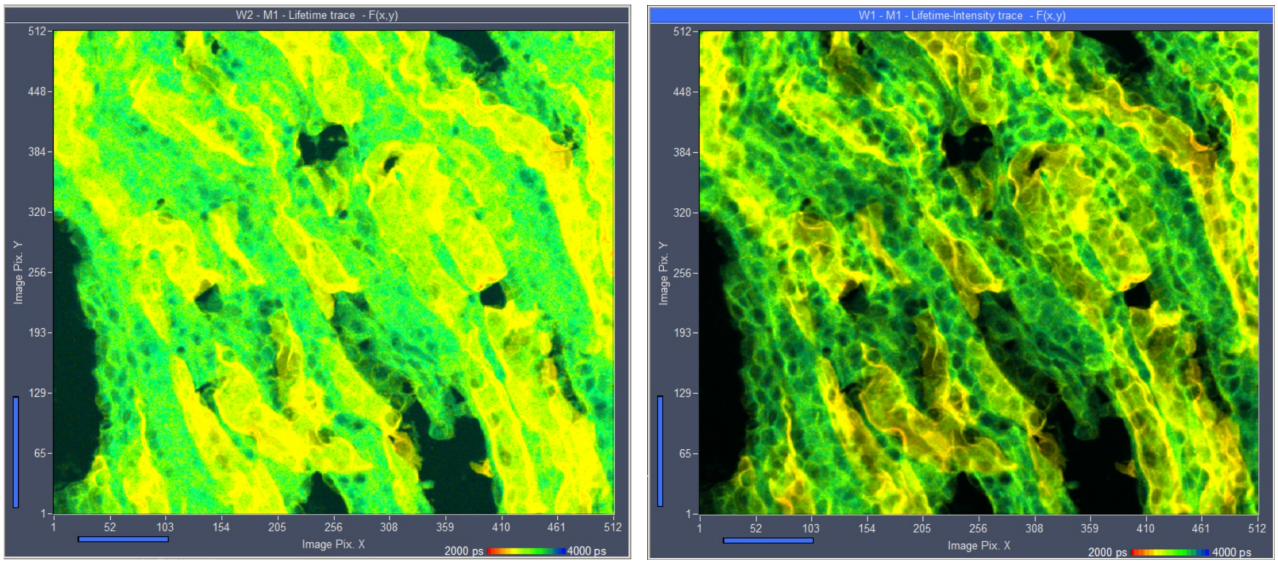

Fig. 30: High-count rate images recorded from an Invitrogen F24630 Mouse kidney section. Left: Traditional FLIM mode. Right: Lifetime/Intensity mode. Average (recorded) count rate 5.5 MHz.

Data Analysis

Data analysis cannot compensate for poor quality of FLIM data if these have been carelessly recorded. However, FLIM data analysis can extract a wealth of information from data which have been recorded from optimally designed samples and with the necessary care [3]. The section below addresses just a few important points and demonstrates them on typical FLIM data.

Which Model?

The first question when it comes to FLIM data analysis is usually: Which model do I have to use? How many exponential components are necessary to fit the results?

The answer does not depend on the number of decay components the sample actually has. It rather depends on what you want to find out from this sample. Therefore, no one except yourself can answer the question. You have a hypothesis of what is going on in a specific biological system. You design an experiment and a sample to confirm or exclude the hypothesis. Only you can know what is expected to happen in your sample, and only you can know how many components are to be expected in the decay functions. Therefore, you should select different models and make sure that the model (and only the model) with the corresponding number of decay components fits the data.

Here is an example. You are doing a protein-interaction experiment. You are using FRET as an indicator of protein interaction. You label one protein with a donor, the other with an acceptor. In places where the proteins interact FRET should occur. FRET reduces the lifetime of the donor. You therefore acquire FLIM data at the donor emission wavelength.

You load the data in SPCImage and run the analysis with a single-exponential model. The fluorescence lifetime is shortest in the cell membrane - exactly where you expect the proteins to interact (Fig. 31, left).

You check the decay functions in a few characteristic spots of the image. In places where the lifetime is short a single-exponential model does not fit the decay functions properly, but a double-exponential one does (Fig. 31, second left). This is plausible: First, not all donor molecules have the right orientation to an acceptor for FRET to occur. Second, protein interaction is a chemical equilibrium, and there should be a mixture of interacting and non-interacting donor. These fractions have different lifetime, consequently the decay profile should be double-exponential.

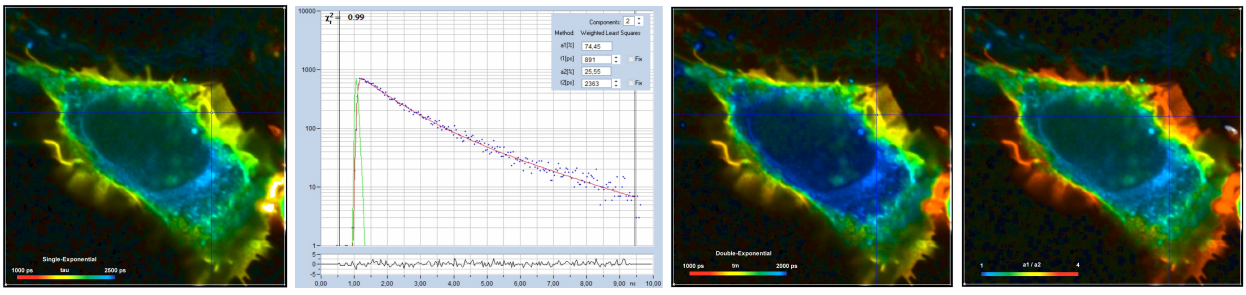

Fig. 31: Results of a FLIM-FRET measurement. Left to right: Single-exponential lifetime image, decay curve at cursor position, image of amplitude-weighted lifetime of double-exponential model, showing classic FRET intensity, image of amplitude ratio, showing relative fraction of interacting proteins.

Now you run data analysis with a double-exponential model. For display, you select the amplitude-weighted mean lifetime, tm. This is the representation of the classic FRET efficiency. The image is shown in Fig. 31, second right. Next, you select the ratio of the amplitude of the fast and the slow decay component. The ratio indicates the relative amounts of interacting and non-interacting donor. It is highest in the cell membrane, where you expect the proteins to interact, see Fig. 31, right. The result shows that a double-exponential model is appropriate to fit the data, and it shows that the initial hypothesis is likely to be correct.

Parameter to be Displayed

SPCImage offers several options to display parameters of the decay functions. Available are the classic single-exponential lifetime, lifetimes of decay components, the amplitude-weighted average and the intensity-weighted average of the component lifetimes, and relative intensities contained in the decay components [3]. SPCImage also displays ratios of these parameters. If possible, a parameter combination should be selected that shows the effect of interest most clearly. For example, in a FRET measurement the amplitude-weighted lifetime of a double-exponential fit, represents the classic FRET efficiency, and the ratio of the amplitudes, a1/a2, the relative fraction of interacting donor. Examples are shown above in Fig. 31.

An examples for metabolic imaging is shown in Fig. 32. The image on the left shows the amplitude ratio of the decay components from free and bound NADH. This parameter characterises the metabolic state of the cells. The images of the component lifetimes, t1 and t2, are shown middle and right. The inhomogeneity of the lifetimes indicates different molecular environment of the NADH in the individual mitochondria.

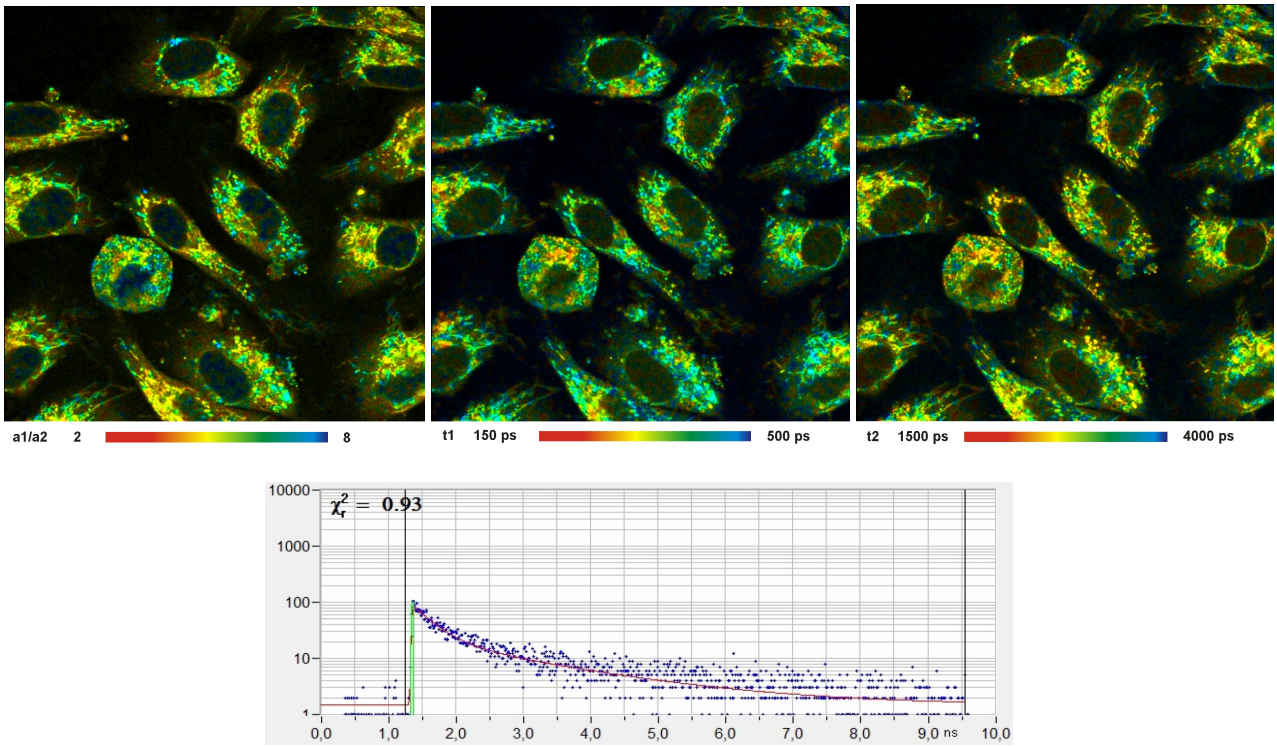

Fig. 32: Left to right: NADH images of live cells. Images of the amplitude ratio, a1/a2 (unbound/bound ratio), and of the fast (t1, unbound NADH) and the slow decay component (t2, bound NADH). FLIM data format 512x512 pixels. Bottom: Decay curve in selected spot. 1024 time channels. time-channel width 10ps.

Binning

Binning of lifetime data is often disapproved of by FLIM users as a way of unscientifically tweaking measurement results. However, correct binning is key to any accurate and reliable FLIM data analysis.

When an image is recorded by an optical system the spatial resolution is limited by diffraction. The diffraction pattern for a single point of light is called Airy disc or (in microscopy) point-spread function. To reach diffraction-limited resolution the data must not be blurred additionally by pixelling. As a rule of thumb, the central disc of the point-spread function should be sampled by about 5 x 5 pixels. Of course, the lifetime information in the pixels within this area is closely the same. It is therefore appropriate to combine the temporal data of these pixels for FLIM analysis, see Fig. 33, left. The result is a substantial increase in the photon number and a corresponding increase in lifetime accuracy. Please note that combining a 5 x 5 pixel area increases of the net photon number by a factor of 25!

In SPCImage binning is performed by combining the data from a defined binning area and assigning the net decay curve to the central pixel. The effective number of pixels in the image is therefore not changed. The procedure also meets an esthetical aspect of a good image. Visually, an image can contain a large amount of intensity noise before it starts to look ugly. The same amount of noise in the lifetime data would, however, render the data useless for any kind of serious FLIM application. It therefore makes sense to display an image at a large number of pixels with some intensity noise, but with the lifetime averaged within larger areas and correspondingly increased signal-to-noise ratio. The principle of binning in SPCImage is illustrated in Fig. 33, right.

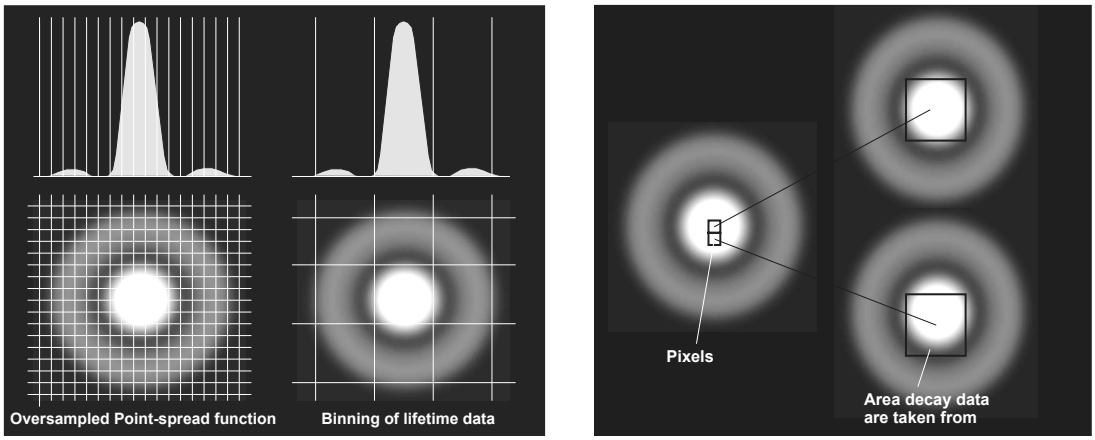

Fig. 33: Left: Oversampling of the Airy disc in the intensity image and binned pixels for lifetime calculation. Right: Overlapping binning of pixels for lifetime calculation.

The meaning of the binning parameter, n, in SPCImage is illustrated in Fig. 34. Please note that a binning factor of two corresponds to a 5 x 5 pixel area, i.e. roughly to the area of the point-spread function in a correctly sampled image. Unintentionally, images are often taken with higher oversampling, especially when high zoom factors of the scanner are used. Therefore SPCImage provides binning factors of up to 10, corresponding to an area of 20 x 20 pixels.

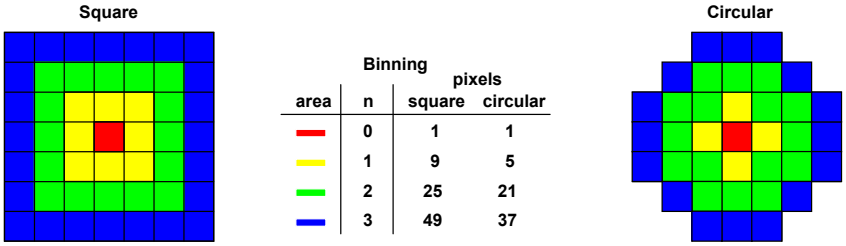

Fig. 34: Function of the binning parameter, n. Binning 'Square' (left) and 'Circular' (right).

A demonstration of the effect of binning is given in Fig. 35. A BPEA sample was scanned with 512 x 512 pixels, the decay curves were recorded into 1024 time channels. Data without binning are shown in the top row of Fig. 35. A (single-exponential) lifetime image is shown on the left. Without binning the number of photons per pixel is ridiculously low, see second left. Consequently, the lifetime image looks noisy, and the decay times scatter all over the place, see lifetime histogram on the right. The bottom row of Fig. 35 shows data analysed with binning. A binning factor of 2 with circular binning was used, corresponding to a binning area of 21 pixels. The lifetime image is of excellent quality, the net decay functions have enough photons for a reasonable fit, and the lifetime histogram has a reasonable width. As can be seen in the image, the colour does not blur out, i.e. binning did not cause noticeable loss in the spatial resolution of the lifetime.

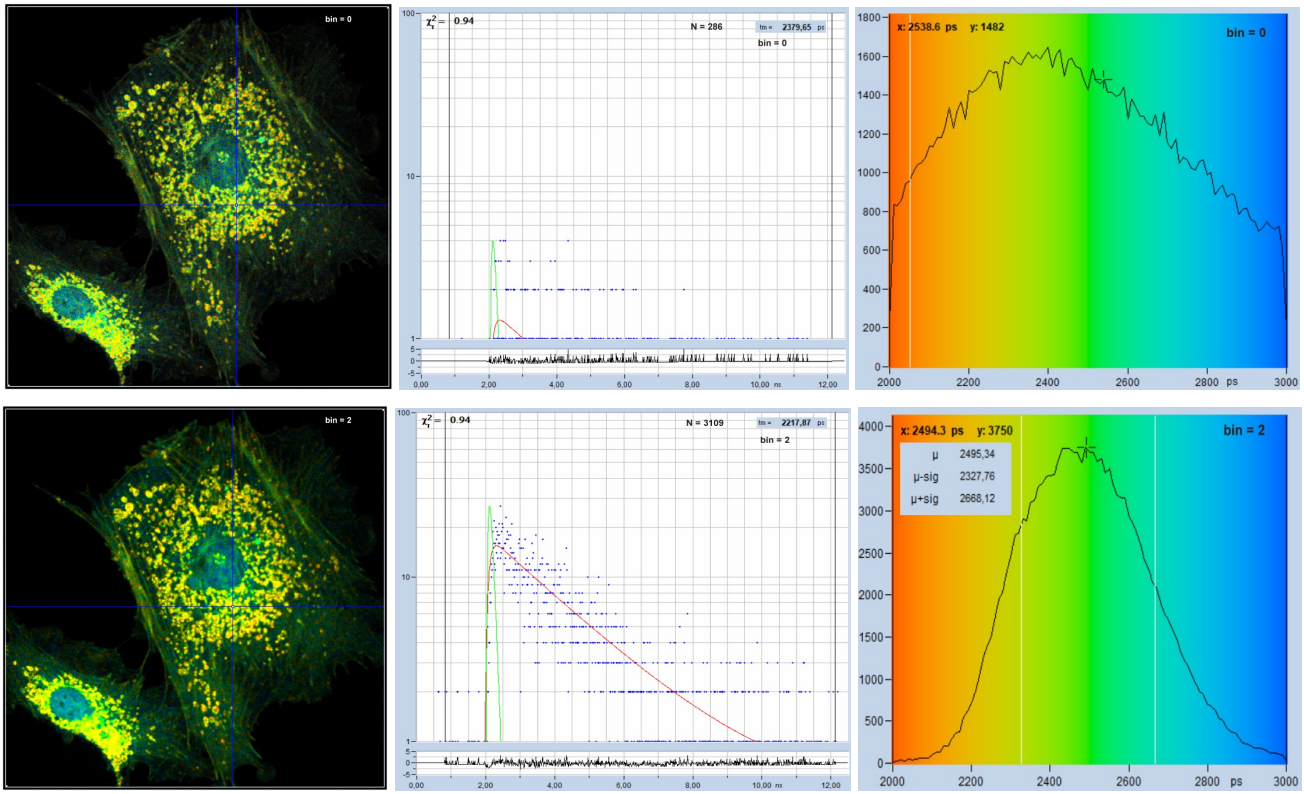

Fig. 35: Effect of binning in lifetime analysis. 512 x 512 pixels, 1024 time channels. Top: No binning. Bottom: Binning factor 2, circular binning. Sum of decay curves of 21 pixel area is used for analysis of central pixel.

With a binning factor of 2 (decay curves from 21 pixels binned into centre pixel, see Fig. 34) the data are even good enough for double-exponential decay analysis. The result is shown in Fig. 36. The top row, left to right, shows lifetime images of the fast decay component and of the slow decay component, and an image of the ratio of the amplitudes of the two components. All three images are of

good quality, both in terms of spatial resolution and lifetime resolution. The bottom row shows the parameter histograms. They show that the component lifetimes and the amplitude ratio are obtained at a good signal-to-noise ratio (please note the different parameter ranges).

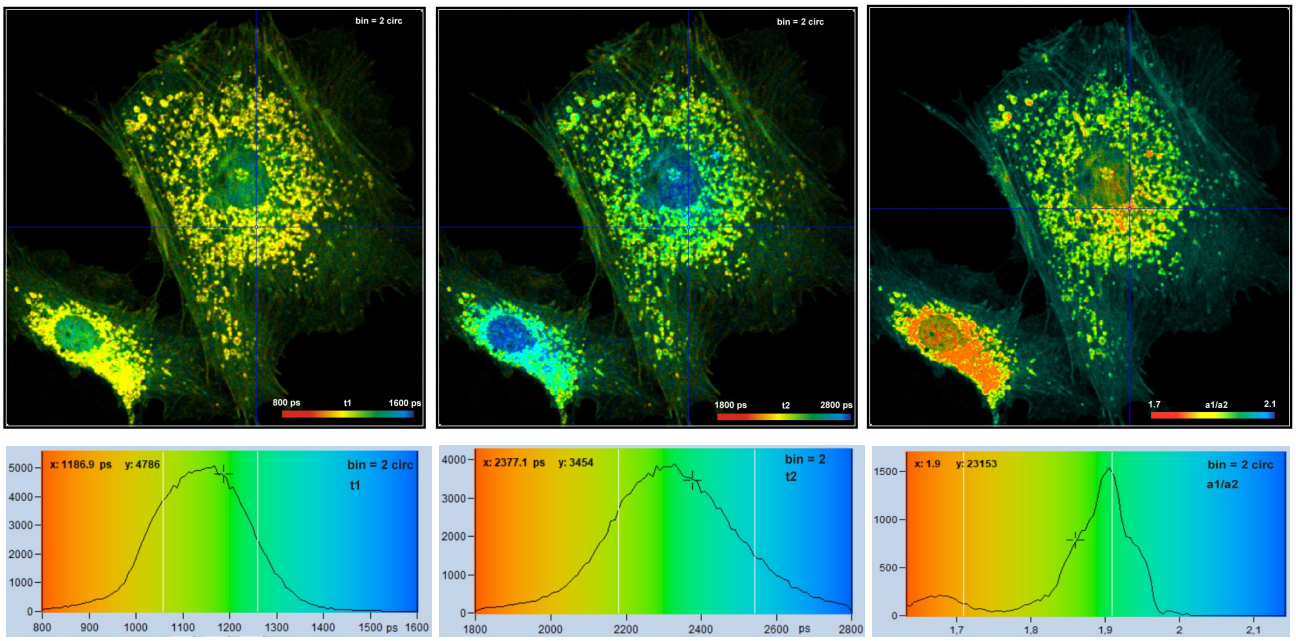

Fig. 36: Same data as in Fig. 35, bottom. Double-exponential decay analysis. Left to right: Lifetime image of fast component, t1, lifetime image of slow component, t2, image of amplitude ratio, a1/a2. Please note different parameter ranges.

Fig. 37 shows the effect of binning on the spatial resolution of the lifetime information. The figure shows data from a 70 x 70 pixel area in the centre of the large cell in Fig. 35 and Fig. 36. As expected, lifetime contrast remains largely unchanged up to binning = 2, see the flower-like structure in the centre. For binning factors of 4 and 6 (second right and right) the lifetime contrast starts to degrade. Too many decay data from adjacent pixels are mixed into the net decay functions. The structure in the middle therefore more and more assumes the lifetime of its closer environment.

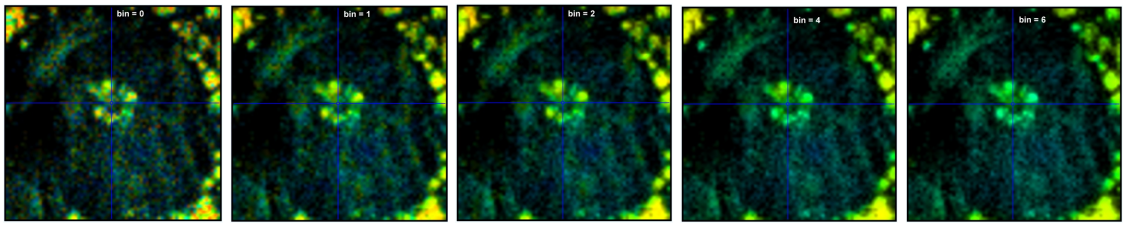

Fig. 37: Zoom into a 70 x 70 pixel area of the data of Fig. 35, showing the centre of the large cell. Different binning, left to right bin = 0, 1, 2, 4, and 6. Lifetime contrast remains unchanged up to bin = 2 (centre image). It degrades at bin = 4 and bin = 6, as can be seen by a fading of the colour of the structure in the centre.

Image Segmentation

In contrast to binning, which combines spatially related pixels, image segmentation combines pixels which have a similar decay signature.

The procedure is shown in Fig. 38. Upper left, Fig. 38 shows the SPCImage panel with FLIM data of low photon number. The data are the same as in Fig. 35, upper row. Decay data in a selected pixel are shown in the lower right of the panel. The lifetime image calculated from these data is noisy, and the histogram of the lifetime (upper right) is extremely wide. The next step is shown in Fig. 38, upper right. A phasor plot is calculated from the data. As expected, the phasors scatter all over the place. Nevertheless, phasors from pixels with distinctly different lifetime (indicated by colour) appear in different phase/amplitude locations.

In a third step, a range of phasor values is selected, and the corresponding pixels are highlighted in the lifetime image, see Fig. 38, bottom left. The selection area can be shifted and changed in size and shape to highlight the desired structures in the image. In the example shown, the mitochondria of the cell have been selected. Even though the selection may be incomplete the selected pixels are all within the desired structures of the image.

In the final step, Fig. 38, bottom right, the decay data of the selected pixels are combined into a single decay curve. This curve contains more than 3 million photons, compared to a few 100 in the individual pixels, and to about 3000 in a binning area of two, compare Fig. 35. A decay curve with 3 million photons can be analysed at high precision. Triple-exponential analysis is no problem, as can be seen in Fig. 38, bottom right. Triple-exponential decay parameters are displayed in the upper right part of the panel.

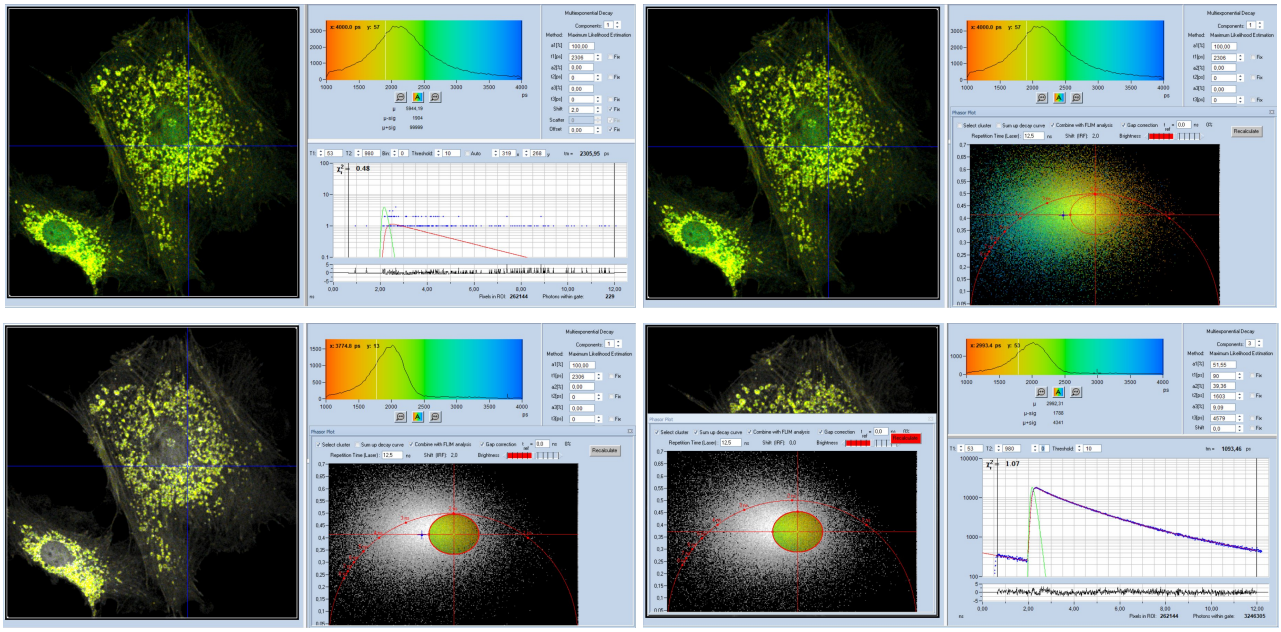

Fig. 38: Image segmentation via the phasor plot, and combination of the selected pixel into a single decay curve of high photon number.

Precision FLIM Analysis of Moving Objects

Motion in the objects to be imaged is a general problem of laser scanning microscopy. It is an even bigger problem for FLIM because it makes it impossible to collect a sufficiently large number of photons for accurate FLIM analyis. As an example, Fig. 39 shows a leg of a live waterflee. The leg is moving quickly so that even single 0.5 s frames become badly distorted. The number of photons

obtained within the 0.5 s frames allows for approximate lifetime determination (see Fig. 39, right) but is insufficient for precision decay analysis.

The solution is 'Temporal Mosaic FLIM' with image segmentation [9]. A series of fast scans is recorded by the Mosaic Imaging function of SPCM. The entire mosaic is loaded into SPCImage. A preliminary data analysis is performed, and the result is loaded into the Phasor Plot. In the phasor plot, a range with the decay signature of the leg is selected. The decay data of all pixels of the selected signature are combined into a single decay curve. This curve contains about five million photons and can be analysed at high precision. Please see Fig. 40. The decay parameters are shown upper right. The parameters of the first tow decay components are characteristic of FAD, the third component even shows a trace of FNM [8].

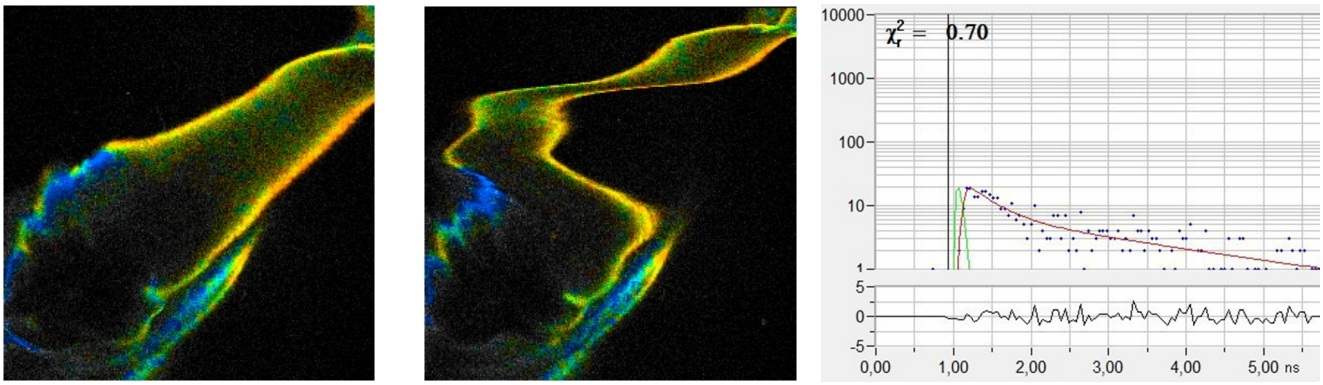

Fig. 39: Left and middle: Moving leg of a live waterflee, 0.5-s scans. Right: decay curve in a spot of 5x5 pixels.

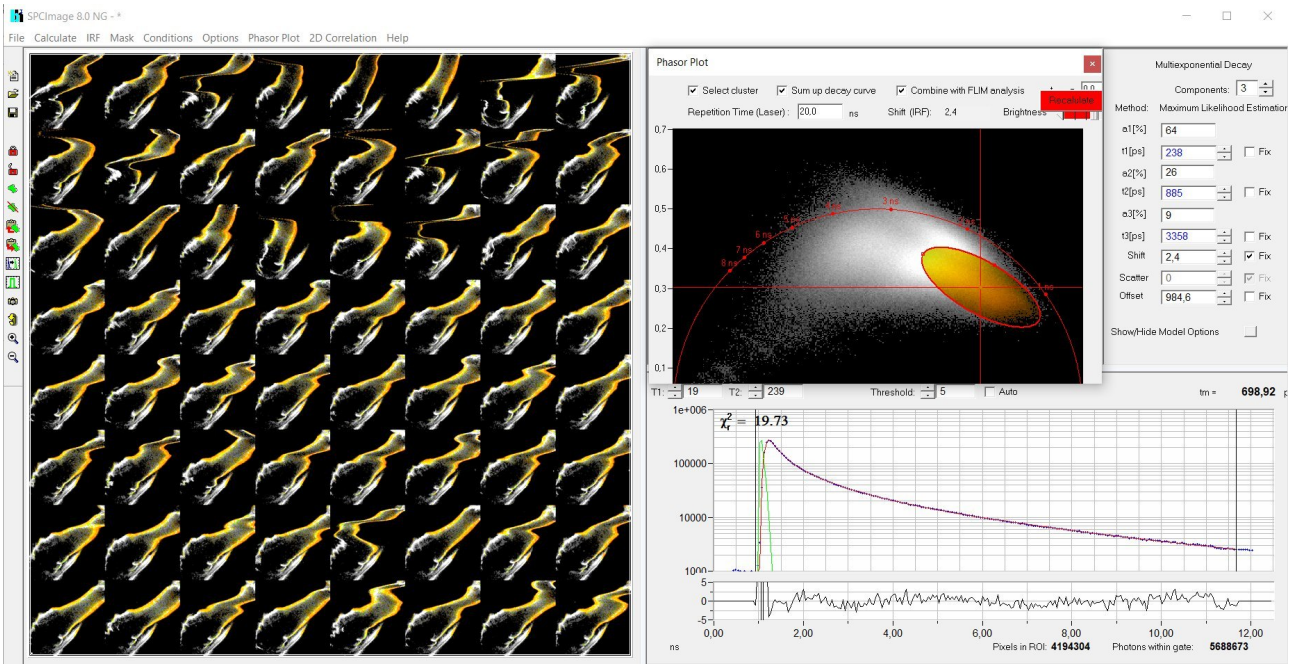

Fig. 40: Left: Temporal Mosaic of the waterflee, 0.5 s per element. Right: Phasor plot. Decay signature of the waterflee leg selected, decay data combined in a single decay curve.

Analysis with Fixed Component Lifetimes

Multiexponential decay analysis becomes easier if the number of decay parameters is reduced. Including a priori knowledge in the data analysis can therefore reduce the noise in the results. Fig. 41 shows an NADH image of an open tumor in a mouse, imaged with the bh DCS-120 MACRO system. The interesting parameter is the amplitude, a1, of the fast decay component. It represents the fraction of free NADH, and indicates the type of the metabolism in the corresponding area of the tissue. The data were therefore analysed with a double-exponential model, and a1 images were created. The image on the left was analysed with all parameters, t1, t2, a1, a2, freely floating. The image on the right was analysed with fixed t2. As expected, the image on the right is less noisy. The tumor stands out more clearly, both in the image and in the a1 histograms. The histogram on the right even displays two distinct populations of pixels, one with a1 = 0.65 and one with a1 = 0.83. These are exactly the amplitudes typically found in healthy tissue and in tumor tissue.

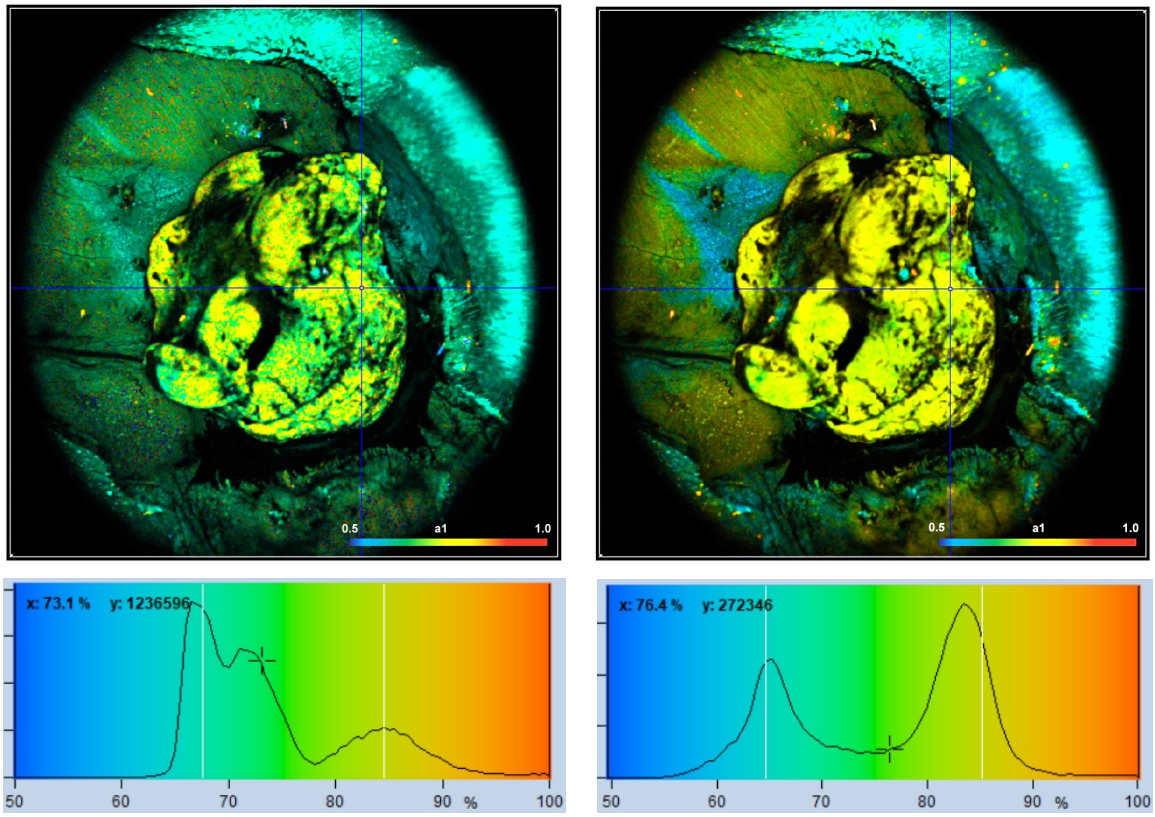

Fig. 41: NADH images of a mouse tumor showing the amplitude, a1, of the fast NADH component. Left: T1, t2, a1, a2 floating. Right: t2 fixed to most frequent value, 2400 ps. Lower row. Histograms of a1 over the pixels of the image.

Analysis with fixed parameters can substantially reduce the noise in cases where lifetimes of decay components are expected to be constant. However, the technique has to be used with caution. Fluorescence lifetimes are never absolutely constant. There is always an influence of the molecular environment. If a component lifetime is fixed but not absolutely constant the fit procedure responds with large changes in other parameters. Therefore, fit results obtained with fixed component lifetimes can have large systematic errors.

The Final Touch: Image Intensity and Parameter Range

A FLIM image should clearly and plainly demonstrate the scientific facts claimed in the associated publication. The images should not only display the right decay parameters but also display them within an appropriate intensity and decay-parameter range. As a default, SPCImage uses autoscaling of the intensity. Under normal circumstances, autoscaling yields reasonable images. However, the autoscale function cannot know which part of the image is the one that contains the information of interest. If the information is in the dim areas of the image autoscaling does not necessarily deliver the best possible image. Also, it can happen that an otherwise perfect image contains a few extremely bright spots. Wherever they come from, autoscaling does not yield a reasonably scaled image in these cases. Autoscaling should therefore be turned off and the intensity scale be adjusted manually. An example is shown in Fig. 42. Autoscaling (left) leads to an unfavourably scaled intensity range. Manual adjustment of the intensity range leads to a correctly balanced image (right).

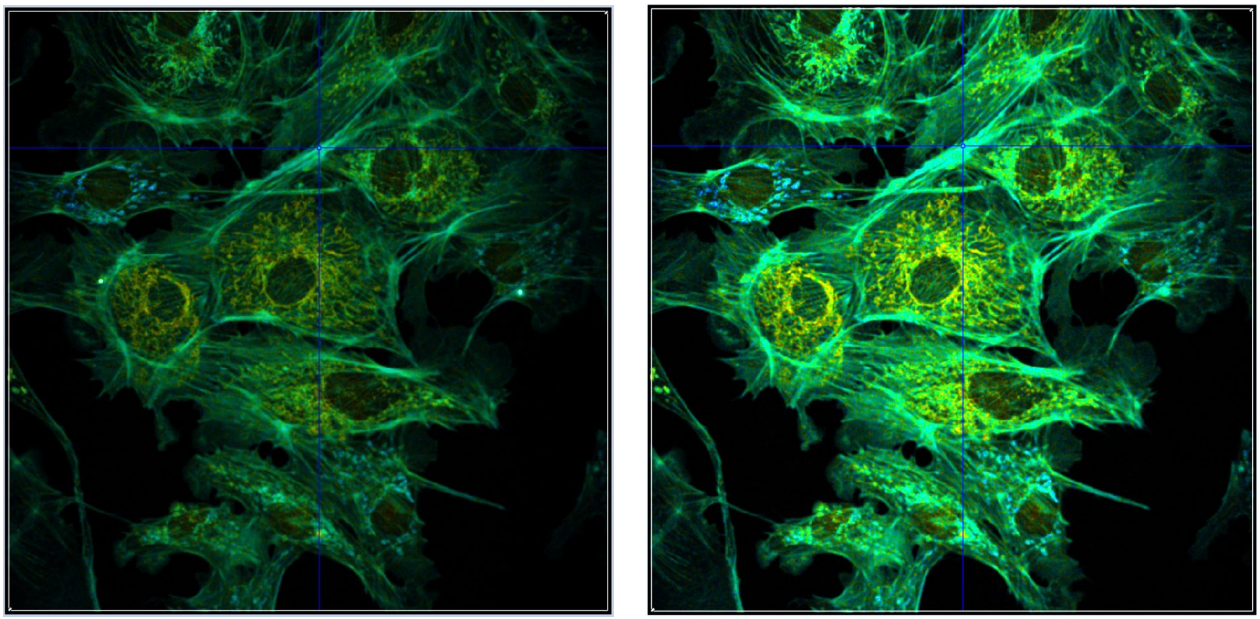

Fig. 42: Image containing a few extremely bright spots. Left: Autoscaling of the intensity range. The autoscaling function scales the intensity to the brightest features. The intensity range obtained is not appropriate for the rest of the image. Right: Manual scaling yields an image within the right intensity range. Lifetime of single-exponential fit, colour range from 2000 ps (blue) to 3000 ps (red)

The display of images with different parameter scale is shown in Fig. 43 and Fig. 44. The figures show lifetime images displayed with a colour direction blue-green-red and red-green-blue, respectively. The parameter ranges are 2000 to 3000 ps (left) and 2300 to 2700 ps (right). Which style displays the effect of interest best must be decided from case to case.

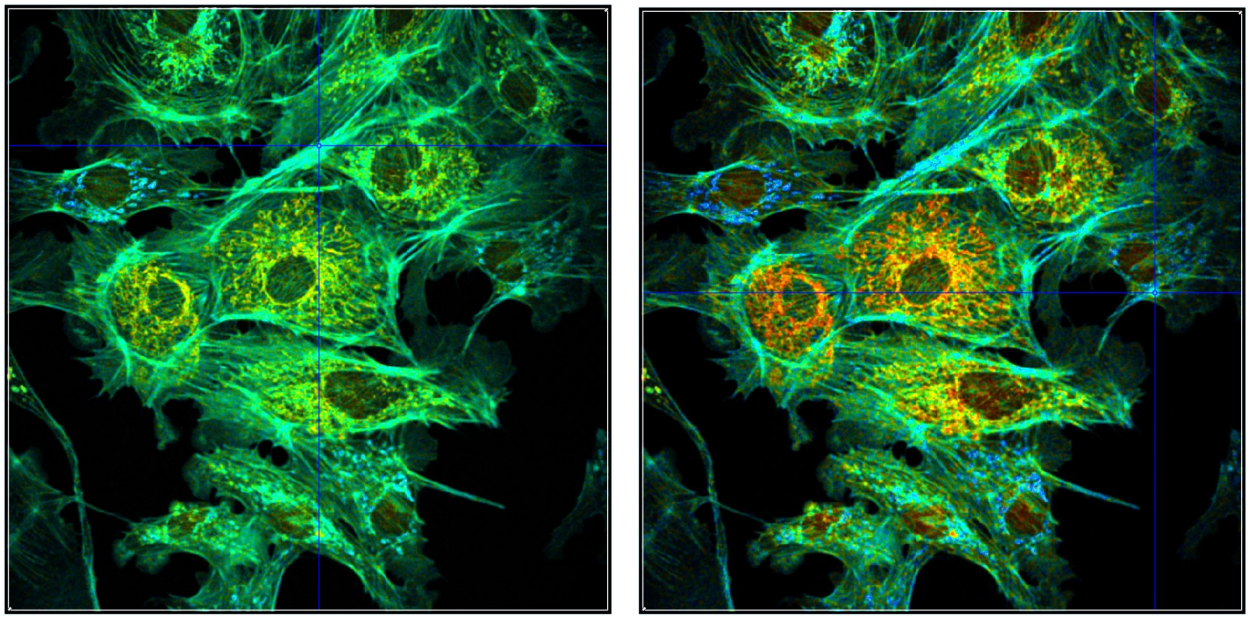

Fig. 43: Different representations of the data shown in Fig. 42. Single-exponential lifetime, manual intensity scaling, colour direction b-g-r. Left: Lifetime range 2000 to 3000 ps. Right: Lifetime range 2300 to 2700 ps.

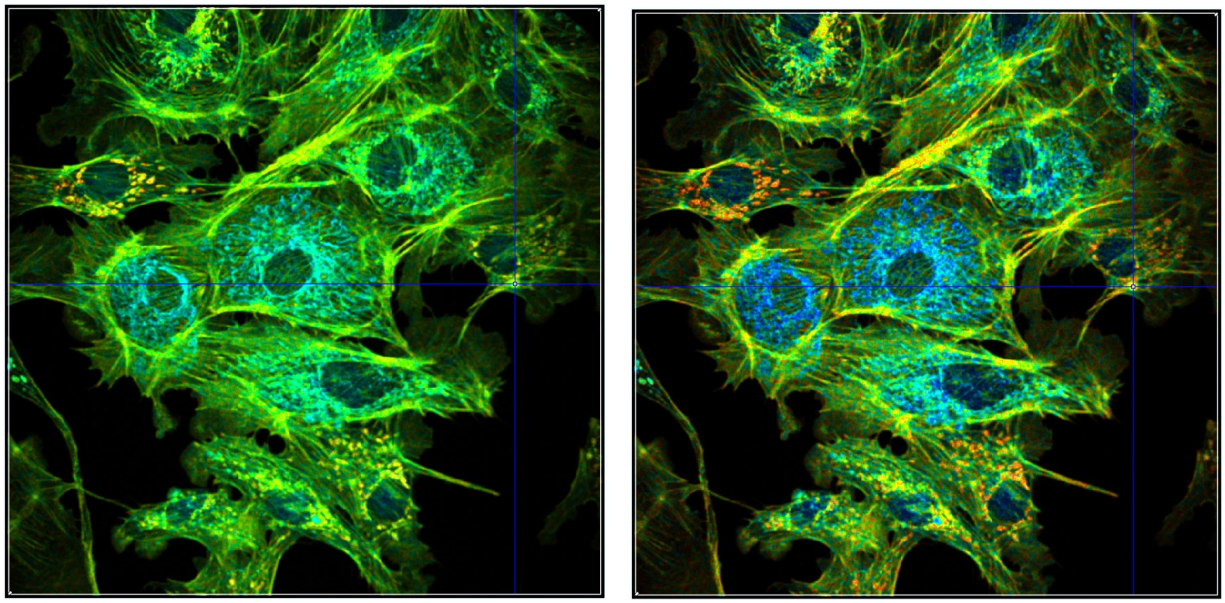

Fig. 44: Different representations of the data shown in Fig. 42. Single-exponential lifetime, manual intensity scaling, colour direction r-g-b. Left: Lifetime range 2000 to 3000 ps. Right: Lifetime range 2300 to 2700 ps.

Summary

The fluorescence lifetime can be derived from TCSPC FLIM data at a signal-to-noise ratio close to square root of the photon number per pixel. Therefore, the most important parameter that characterises FLIM data quality is photon number. By using practical examples, we have shown that by simply optimising the detection efficiency and the acquisition time a factor of 10 in photon number can be gained. By using high-efficiency detectors another factor of 4 can be added, and optimised binning strategies can add a factor of 25. Altogether, this is a factor of 1000 in photon number, or a factor of 32

in signal-to-noise ratio. We do not claim that an improvement this large can be reached in all cases, but a sizable improvement is achievable almost anytime.

The second important parameter of a FLIM system is photon efficiency. Photon efficiency describes how efficiently the individual photons detected by the system contribute to the result. In other words, it describes how close the system gets to the ideal signal-to-noise ratio, SQRT(N). Although TCSPC systems come close to the ideal, the photon efficiency can often be optimised by using the correct TCSPC timing parameters, by avoiding the recording of background signals, and by using sufficiently fast detectors. Often an increase by a factor of two to four in photon efficiency is possible by just obeying to a few simple rules of signal recording.

Data quality becomes especially important when multi-exponential decay functions are recorded and analysed. In the most frequent FLIM applications multi-exponential decays are rather the rule than the exception. The information is then primarily in the amplitudes and lifetimes of the decay components rather than in the apparent lifetime of the net decay functions. That means not only detection efficiency and photon efficiency are important but also the width of the instrument-response function. Moreover, the options of resolving multi-exponential decay functions dramatically depend of the shape of the decay functions. The more they deviate from a single exponential profile the better they can be resolved. Therefore, experiment planning and sample design with the options of FLIM in mind can have a massive influence on the outcome of a research activity.

Finally, data analysis plays an important role in any FLIM experiment. Correctly applied data analysis can extract a maximum of information from data which have been recorded with the precautions outlined in this brochure. Moreover, it is able to present the data in publication-ready style, and in a form that convincingly supports the claims made in the associated publication.

Examples of Beautiful FLIM Images

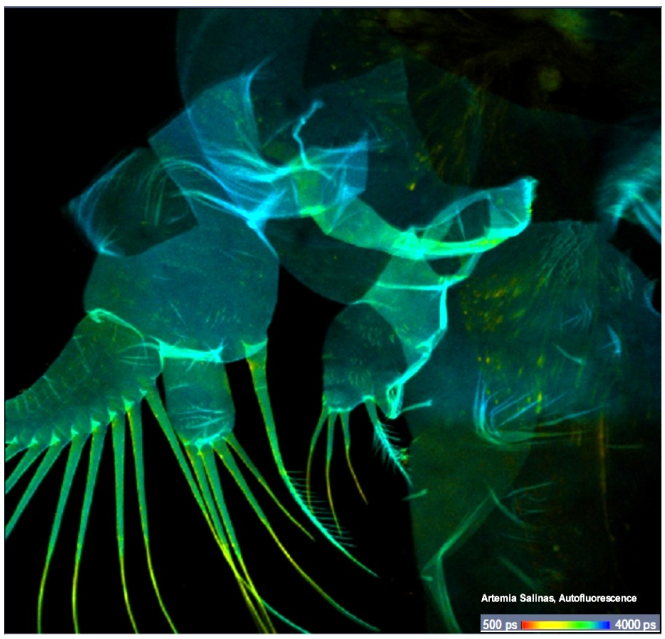

Artemia Salinas, Autofluorescence, DCS-120 Confocal

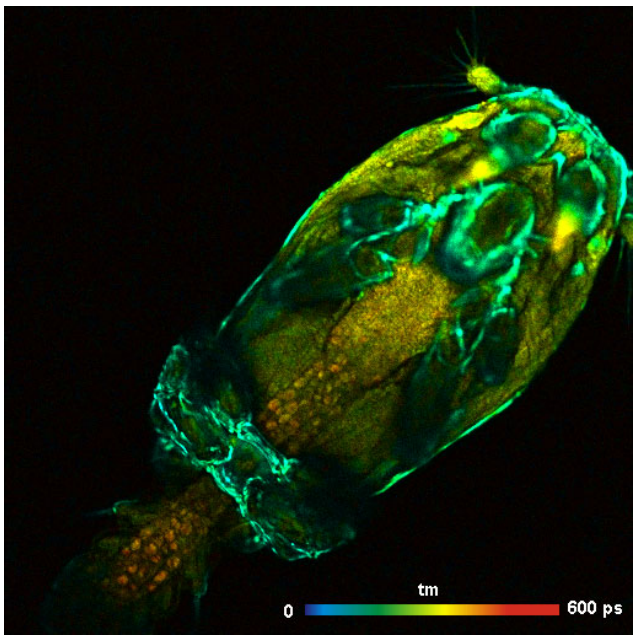

Salmon Louse, bh FLIM on Sutter MOM microscope

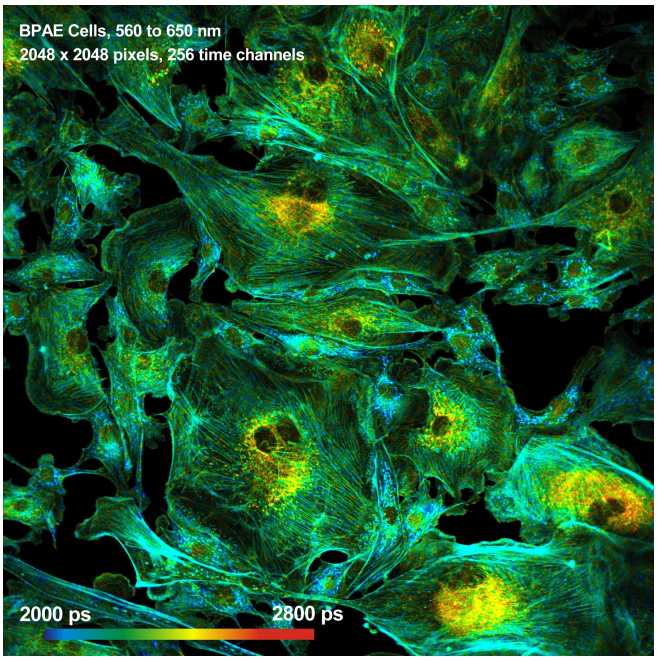

Bovine pulmonary artery cells, 560 nm, DCS-120 confocal

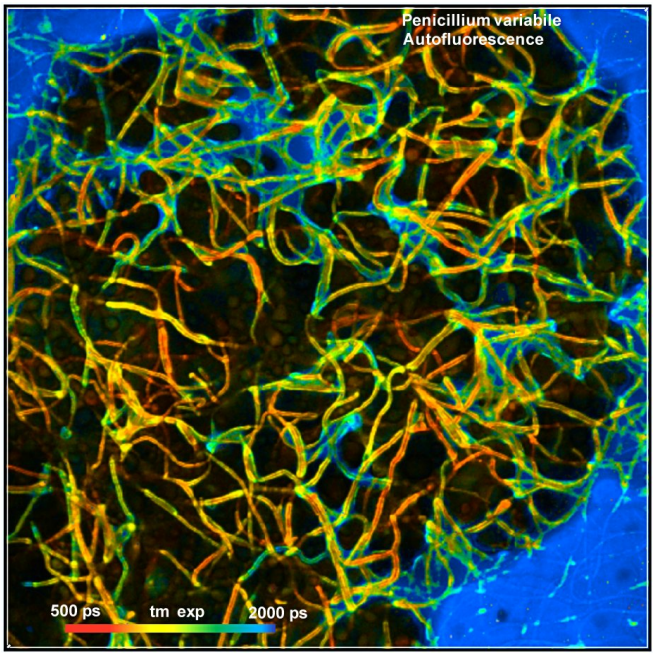

Penicillium variabile, DCS-120 confocal

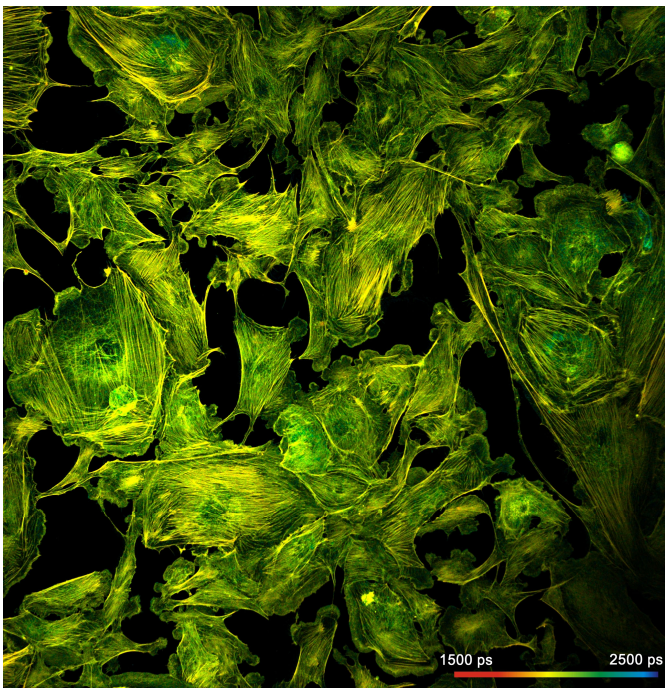

Bovine pulmonary artery cells, 480 nm, DCS-120 confocal

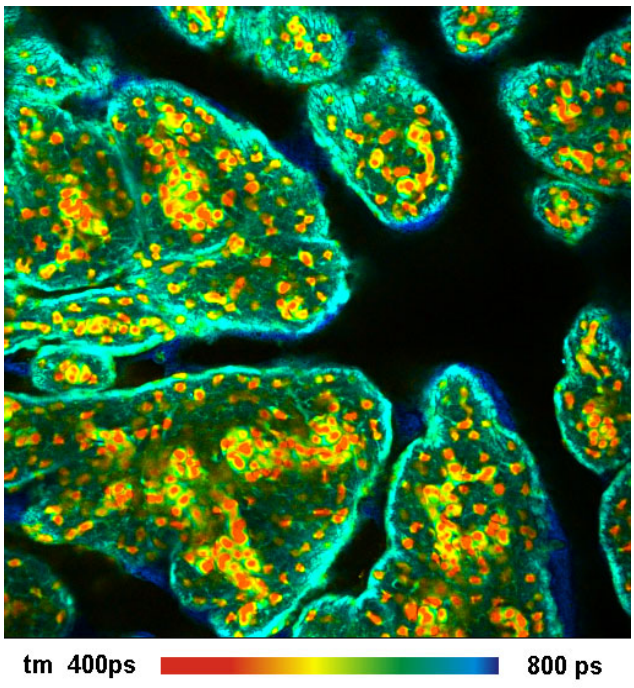

Pig skin, stained with methylene blue, Zeiss LSM 880 NLO

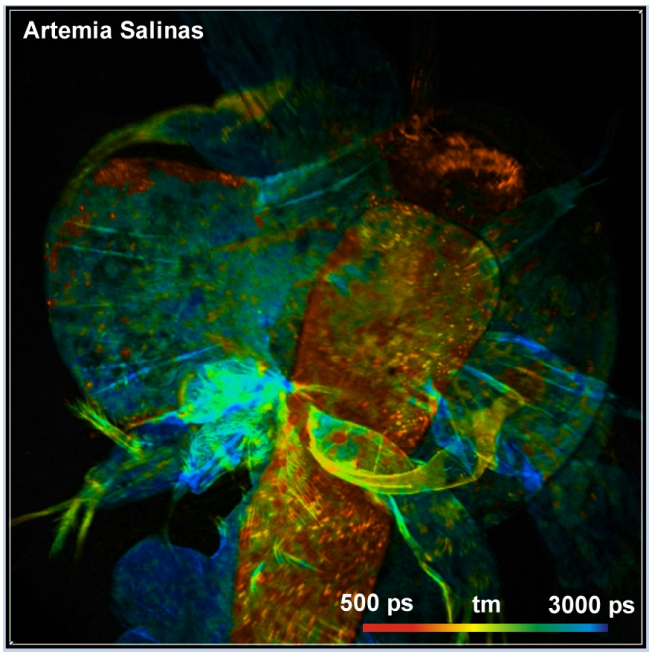

Artemia Salinas, Autofluorescence, DCS-120 MP

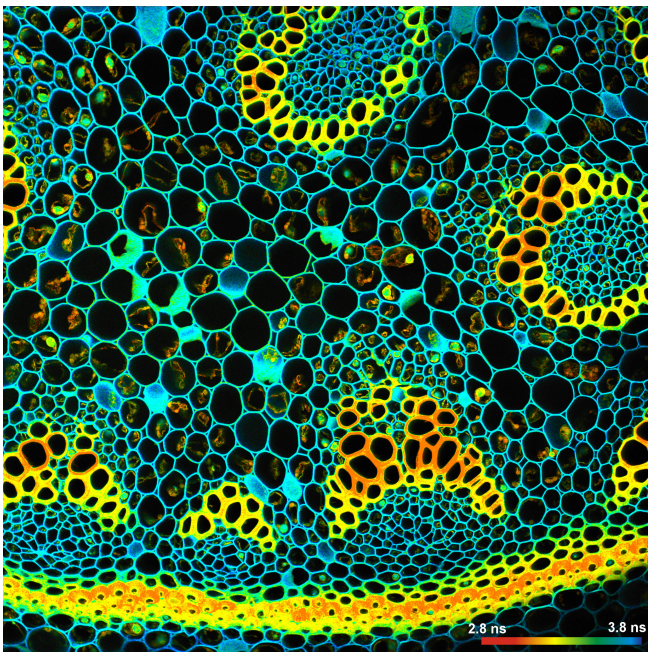

Convallaria sample, Zeiss LSM 780 NLO

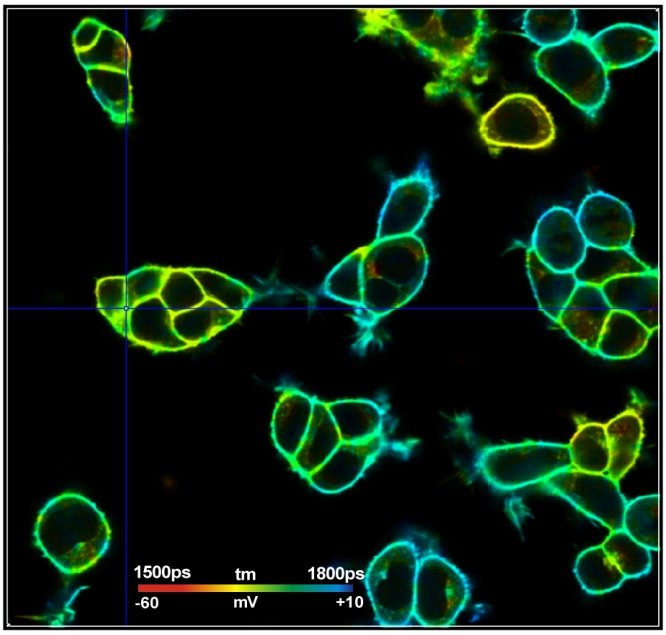

Membrane potential of HEK cells. Zeiss LSM 980

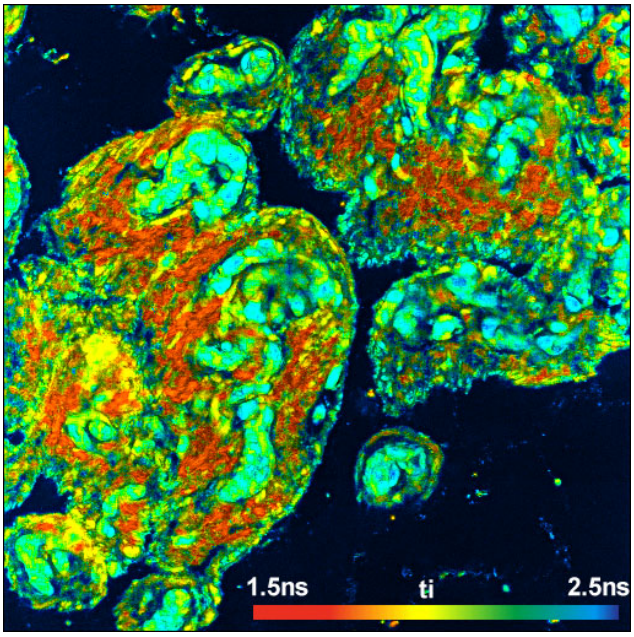

Pig Skin, autofluorescence. Leica SP8 with HyD detectors

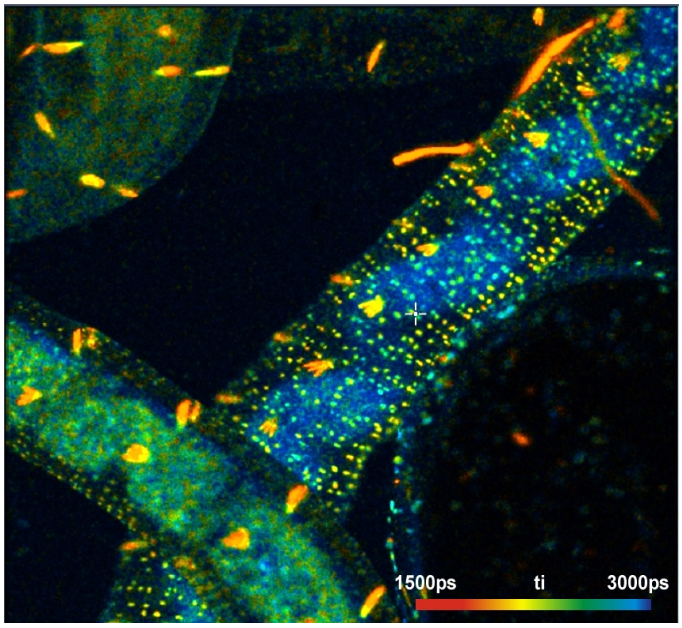

Enchytraeus albidus, autofluorescence, 1 s aqusition time, DCS-120 with SPC-QC-104.

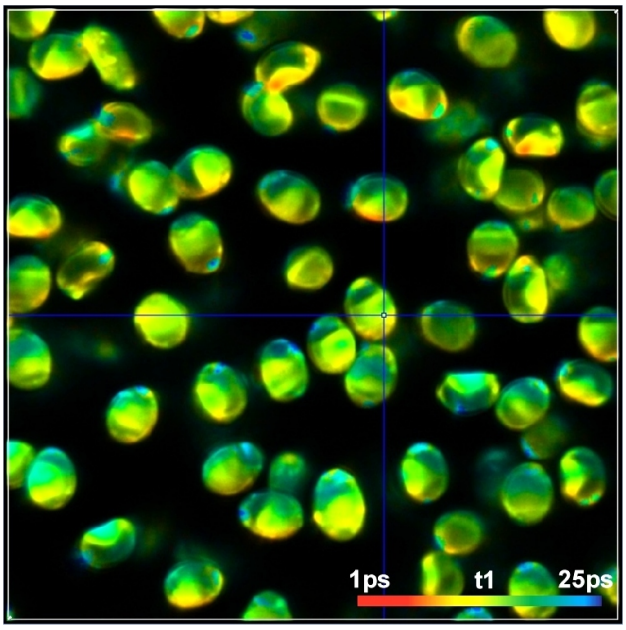

Spores of paxillus involutus. Ultra-fast decay. Average t1 is 12.5 ps. DCS-120 MP system.

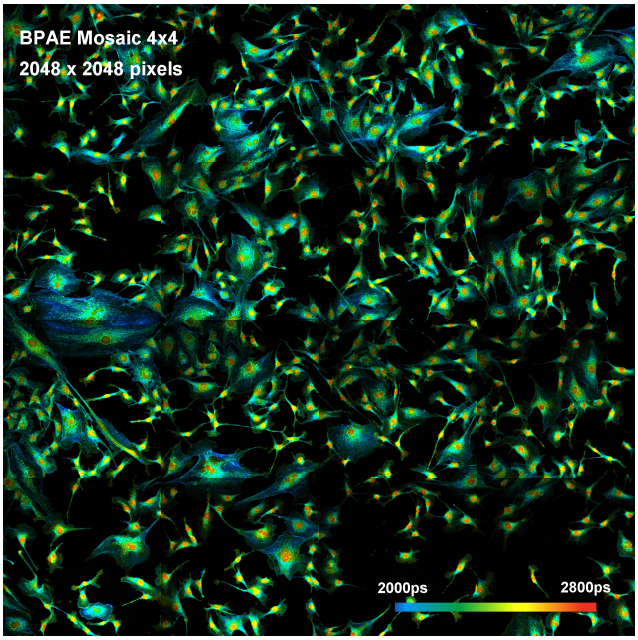

Mosaic FLIM image of BPAE cell sample. DCS-120 MP

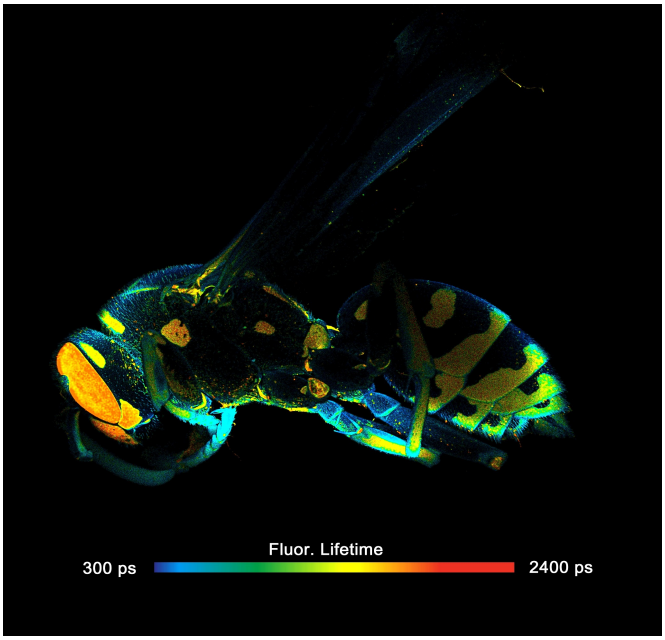

FLIM Image recorded with DCS-120 MACRO system

References

1. W. Becker, Advanced time-correlated single-photon counting techniques. Springer, Berlin, Heidelberg, New York, 2005
2. W. Becker, The bh TCSPC handbook, 9th edition. Becker & Hickl GmbH (2019), available online on www.becker-hickl.com. Please contact bh for printed copies.
3. SPCImage NG data analysis software. In: W. Becker, The bh TCSPC handbook, 9th edition. Becker & Hickl GmbH (2019)
4. W. Becker (ed.), Advanced time-correlated single photon counting applications. Springer, Berlin, Heidelberg, New York (2015)
5. Becker & Hickl GmbH, DCS-120 Confocal and Multiphoton Scanning FLIM Systems, user handbook 87th ed. (2019). Available on www.becker-hickl.com
6. Becker & Hickl GmbH, Modular FLIM systems for Zeiss LSM 510 and LSM 710 family laser scanning microscopes. User handbook. Available on www.becker-hickl.com
7. Becker & Hickl GmbH, FLIM systems from Zeiss LSM 980 Laser scanning microscopes, addendum to modular FLIM systems for Zeiss LSM 510 and LSM 710 family laser scanning microscopes. Available on www.becker-hickl.com
8. W. Becker, L. Braun, DCS-120 FLIM System Detects FMN in Live Cells. Application note, available on www.becker-hickl.com
9. W. Becker, A. Bergmann, Precision fluorescence-lifetime Imaging of a moving object. Application note, available on www.becker-hickl.com
10. W. Becker, A. Bergmann, M. Schubert, S. Smietana, Lifetime-intensity mode delivers better FLIM images. Application note, available on www.becker-hickl.com
11. Fast-Acquisition TCSPC FLIM: What are the Options? Application note, available from www.becker-hickl.com
12. W. Becker, V. Shcheslavkiy, S. Frere, I. Slutsky, Spatially Resolved Recording of Transient Fluorescence-Lifetime Effects by Line-Scanning TCSPC. Microsc. Res. Techn. 77, 216-224 (2014)
13. R.M. Ballew, J.N. Demas, An error analysis of the rapid lifetime determination method for the evaluation of single exponential decays, Anal. Chem. **61**, 30 (1989)
14. W. Becker, B. Su, K. Weisshart, O. Holub, FLIM and FCS Detection in Laser-Scanning Microscopes: Increased Efficiency by GaAsP Hybrid Detectors. Micr. Res. Tech. 74, 804-811 (2011)
15. Wolfgang Becker, Cornelia Junghans, Axel Bergmann, Two-photon FLIM of mushroom spores reveals ultra-fast decay component. Application note, available on www.becker-hickl.com.
16. Becker & Hickl GmbH, Ultra-fast HPM detectors improve NADH FLIM. Application note, www.becker-hickl.com
17. Becker & Hickl GmbH, Two-Photon FLIM with a Femtosecond Fibre Laser. Application note, www.becker-hickl.com
18. Becker Wolfgang, Suarez-Ibarrola Rodrigo, Miernik Arkadiusz, Braun Lukas, Metabolic Imaging by Simultaneous FLIM of NAD(P)H and FAD. Current Directions in Biomedical Engineering 5(1), 1-3 (2019)
19. H.C. Gerritsen, M.A.H. Asselbergs, A.V. Agronskaia, W.G.J.H.M. van Sark, Fluorescence lifetime imaging in scanning microscopes: acquisition speed, photon economy and lifetime resolution, J. Microsc. 206, 218-224 (2002)
20. M. Köllner, J. Wolfrum, How many photons are necessary for fluorescence-lifetime measurements?, Phys. Chem. Lett. 200, 199-204 (1992)
21. I. Isenberg, R.D. Dyson, The analysis of fluorescence decay by a method of moments. Biophys. J. 9, 1337-1350 (1969)

Contact:

Wolfgang Becker
Becker & Hickl GmbH
Berlin, Germany
Email: becker@becker-hickl.com